NACA

RESEARCH MEMORANDUM

ANALYSIS OF LIMITATIONS IMPOSED ON ONE-SPOOL TURBOPROP-ENGINE DESIGNS BY COMPRESSORS AND TURBINES AT FLIGHT MACH NUMBERS OF 0, 0.6, AND 0.8

By Richard H. Cavicchi

Lewis Flight Propulsion Laboratory
Cleveland, Ohio

NATIONAL ADVISORY COMMITTEE
FOR AERONAUTICS
WASHINGTON

December 6, 1956
Declassified October 31, 1958

NATIONAL ADVISORY COMMITTEE FOR AERONAUTICS

RESEARCH MEMORANDUM

ANALYSIS OF LIMITATIONS IMPOSED ON ONE-SPOOL TURBOPROP-ENGINE DESIGNS BY COMPRESSORS AND TURBINES AT FLIGHT MACH NUMBERS OF 0, 0.6, AND 0.8

By Richard H. Cavicchi

SUMMARY

A design-point analysis of one-spool turboprop engines was made to determine the relations among engine, compressor, and turbine design parameters in order to reveal the primary limitations on turboprop-engine design. For this investigation, sea-level operation and flight at Mach numbers of 0.6 and 0.8 at the tropopause were studied. High aerodynamic limits were assumed for all the turbines considered. No allowance was made for turbine cooling.

Turbine centrifugal stress at the turbine rotor exit was found to be a limiting factor for all flight conditions studied. Increasing the compressor pressure ratio relieves the turbine centrifugal stress. This stress was found to be more severe for sea-level designs than for design conditions of subsonic flight at the tropopause. It appears desirable to strive for high compressor pressure ratios at low tip speeds and low compressor weight flows per unit frontal area. Except for sea-level Mach 0.6 designs at a turbine-inlet temperature of 1668° R, turbines of 30,000 pounds per square inch of stress at the design point are capable of driving light, compact, high-speed compressors. They do so, however, at sacrifices in specific fuel consumption compared with turbines with a stress of about 50,000 pounds per square inch. Furthermore, negligible propeller thrust is available from many engines in which turbines of 30,000-pound-per-square-inch stress are capable of driving light, compact, high-speed compressors.

An increase in turbine-inlet temperature is accompanied by an increase in turbine centrifugal stress. If means are found to raise turbine stress limits above 50,000 pounds per square inch, the primary limitation might shift to the compressor, for compressor aerodynamics becomes a severe problem.

INTRODUCTION

At the present time, subsonic flight can be accomplished with lower specific fuel consumption by craft powered by turboprop engines than by

turbojet engines. The main reason for this is the high propulsive efficiency realized by the propeller, which handles a large mass of air at low velocity.

This report presents a design-point analysis of one-spool turboprop engines in which turbine aerodynamics, compressor aerodynamics, turbine blade centrifugal stress, and engine geometry are related. The object of this report is to reveal the limitations imposed upon turboprop engines by these factors. This study pertains only to engines at their design points, no consideration having been given to the off-design problem.

4078

The analysis developed herein is presented in the form of design-point charts for one-spool turboprop engines. Evaluation of the engine designs is made in terms of engine horsepower and specific fuel consumption. Engine temperature ratios from 3.0 to 6.82 and flight conditions at Mach numbers of 0 and 0.6 at sea level and 0.6 and 0.8 at the tropopause are studied. Compressor pressure ratios from 3 to 40 are considered. Although turbine-inlet temperatures up to 3000° R are considered, no study is made herein of the effects of turbine cooling.

GENERAL CONSIDERATIONS IN ANALYSIS

The charts in this report are intended to facilitate the evaluation of turboprop engines. A schematic sketch of a turboprop engine is shown in figure 1. The following brief discussion reviews the factors involved in making an evaluation. First of all, a primary engine consideration is to have high horsepower and low specific fuel consumption. Selection of such a design, however, must be tempered by compromises in the choices of the following factors.

Turbine Centrifugal Stress

For a given turbine-inlet temperature, higher stresses can be tolerated at the rotor exit of a turboprop engine than at the exit of a turbojet engine. The reason for this is the lower turbine-exit temperature of the turboprop engine, resulting from the higher turbine work output needed to drive the propeller. A stress of 30,000 pounds per square inch at the rotor exit would probably be considered low in a turboprop engine. An engine with such a turbine might be suitable as a "workhorse" engine where a conservative and reliable design is needed for long engine life. In the present study, turbine stresses in the first stage are not evaluated.

Since temperatures are high in this region, it is possible that the stresses in the first stage might become a problem even though they are considerably lower than the exit stresses. Nevertheless, the exit stress is considered a good criterion of the severity of the turbine stress problem, and it is therefore used in this report.

Compressor Aerodynamics

Consideration of compressor aerodynamics is easily projected into this analysis by the use of a parameter e. This parameter, initially reported in reference 1, together with the compressor pressure ratio is indicative of the severity of compressor aerodynamics. Parameter e is defined as

$$e = mc^2 \tag{1}$$

All symbols are defined in appendix A. Figures 2 and 3, discussed in appendix B, show the relations of parameter e_C with rotor inlet relative Mach number, equivalent tip speed, and equivalent specific air flow of the compressor. Low values of e_C are obtained from subsonic compressors, and high values from supersonic compressors. In order to utilize the capacity of the advanced compressors of small diameter, the turbine must operate at high stress. The following table, taken from figure 3(a), lists the minimum values of compressor rotor inlet relative Mach number M_1 for several values of parameter e_C:

M_1	e_C, lb/sec^3
0.9	21×10^6
1.0	27.5
1.1	35.5
1.2	44
1.3	54
1.4	65

A value of 44×10^6 pounds per second^3 for e_C is currently at the fringe of multistage-compressor designs of good efficiency. For this value of e_C, the minimum relative Mach number obtainable at the compressor inlet is 1.2. As shown in figure 2, compressor designs having inlet relative Mach numbers higher than 1.2 are possible at 44×10^6 pounds per second^3. A compressor designer might very well have reasons for choosing designs off the dotted curve of figure 2.

In any event, if the designer were to minimize compressor-inlet relative Mach number M_1 for a value of e_C of 44×10^6 pounds per second^3, figure 3(a) shows that a value of 33.2 pounds per second per square foot

4078
CU-1 back

is obtained for m_C. For the same compressor design, figure 3(b) shows that the compressor equivalent tip speed is 1155 feet per second. Compressor equivalent centrifugal stress for this case is read on figure 2, and it is 42,000 pounds per square inch. This would be the absolute centrifugal stress for sea-level static designs ($\theta_1' = 1$). For other flight conditions, the 42,000 pounds per square inch must be multiplied by θ_1' to obtain the absolute stress.

If, for a value of 44×10^6 pounds per second^3 for e_C, any other tip speed than 1155 feet per second is used (either higher or lower), compressor-inlet relative Mach number is greater than 1.2. If, for example, an equivalent tip speed of 1250 were selected, the compressor-inlet relative Mach number would rise to about 1.22 (fig. 2). 4078

Raising e_C while maintaining minimum M_1 raises the compressor equivalent specific air flow m_C (fig. 3(a)). This means that the compressor diameter decreases for a given air flow. Furthermore, raising e_C, with M_1 a minimum, is accompanied by a rise in compressor equivalent blade tip speed (fig. 2), thus requiring fewer compressor stages for a given compressor pressure ratio. This means that the compressor length decreases. High values of e_C, therefore, mean light and compact compressors. High values of parameter e_C are possible only if the turbine can operate at high stress and the compressor at high Mach numbers.

In the section RESULTS AND DISCUSSION, in which the use of the charts is illustrated, a value of 44×10^6 pounds per second^3 for e_C is used as a base value.

In appendix B it is shown that

$$e_T = (1 + f)(1 - b)e_C \tag{B15}$$

For specified values of fuel-air ratio f and compressor bleed b, parameters e for compressors and turbines are related by a constant factor. If the fuel-air ratio and bleed are small, little error is made in assuming that parameters e for compressors and turbines are equal. In the computations of the present analysis, however, the value of f determined by equation (B2) was used along with zero bleed. Parameter e is thus both a compressor and a turbine aerodynamic parameter. For the turbine, high e is indicative of high turbine tip speed and, hence, high turbine stress for a specified value of weight flow per turbine frontal area.

4078

Turbine Aerodynamics

Limiting turbine work output occurs at a turbine-exit axial Mach number of approximately 0.7, depending upon the trailing-edge blockage of the last rotor blade. All the turbines in this analysis are at the limiting-loading condition.

Parameter e_T is also a turbine aerodynamic parameter. This is seen since

$$e_T = m_T c_T^2$$

In this equation, both m_T and c_T are indicative of the severity of turbine aerodynamics. Parameter e_T, however, cannot be tied together so neatly with turbine-inlet relative Mach number in the manner that e_C corresponds to compressor-inlet relative Mach number. The presence of the turbine-inlet stator eliminates this possibility. Furthermore, since e_T is defined in terms of compressor-inlet stagnation conditions rather than turbine-inlet stagnation conditions, a simple relation between e_T and turbine rotor inlet relative Mach number is not shown.

Engine Geometry

All turbines considered in the present analysis have been assigned a hub-tip radius ratio of 0.5 at the rotor exit. Therefore, when the exhaust-nozzle and turbine frontal areas are equal, the exhaust nozzle is 4/3 as large as the turbine-exit annulus. In this analysis, engine geometry is presented as the ratio of exhaust-nozzle to turbine frontal area.

Presentation of Analysis

The analysis is presented in the form of design-point charts for the various flight conditions selected. The parameters plotted in the charts include specific fuel consumption, engine horsepower per turbine frontal area, turbine blade centrifugal stress, compressor and turbine pressure ratios, compressor parameter e_C, turbine-limited specific weight flow, and the ratio of exhaust-nozzle to turbine frontal area. The basis of the analysis and the manner of constructing the charts are presented in appendix B.

No values lower than 0.705 are shown for the curves of constant A_E/A_T. The value 0.705 occurs when the exhaust nozzle chokes, assuming

an average value of 4/3 for k. Beyond the choking value of exhaust-nozzle pressure ratio, A_E/A_T remains at 0.705, since $(\rho V_x/\rho' a'_{cr})_4$ is assumed constant throughout this analysis.

RESULTS AND DISCUSSION

Sea-Level Static Designs

Charts I and II have been constructed for sea-level static designs with turbine-inlet temperatures of 2075° and 2593° R, respectively. A glance at chart I(b) immediately fixes the region of prime interest in a small section. This, of course, is the compressor pressure ratio curve of 10 at and to the left of the peak. Such designs yield highest horsepower per turbine frontal area and lowest specific fuel consumption. Compressor pressure ratios higher than 10 are not shown on chart I(b) because such curves would lie below the curve of p'_2/p'_1 of 10.

Chart I(b), which was constructed for an inlet temperature of 2075° R, shows that for lowest specific fuel consumption the ratio A_E/A_T is greater than unity. This is also true if the turbine-inlet temperature is raised to 2593° R (chart II(b)).

Use of the charts is illustrated by considering point A, located on chart I(b) by a value of 1.1 for A_E/A_T on the compressor pressure ratio curve of 10. The same point A is also located on the right side of chart I(a). The relative balance between severity of turbine stress and compressor aerodynamics is then revealed by the left side of chart I(a). If a turbine to drive the engine of point A is limited to a stress of 30,000 pounds per square inch at the rotor exit, the compressor that the turbine is capable of driving runs at an e_C of only 26.0×10^6 pounds per second^3 (point A_1). If the tolerable turbine stress is 50,000 pounds per square inch, however (point A_2), the turbine is capable of driving a compressor with e_C of 43.3×10^6 pounds per second^3.

Thus, if tolerable turbine stress can be raised from 30,000 to 50,000 pounds per square inch, the turbine can drive a compressor of 67 percent greater equivalent specific air flow if compressor tip speed is unchanged. A smaller-diameter compressor would result from the reduction in compressor frontal area for a given weight flow. Or, alternatively, if m_C is held fixed, compressor equivalent tip speed can be increased by 29 percent. Such a compressor would be shorter, since the higher tip speed reduces the required number of compressor stages. In any event, the compressor designer has the freedom to apportion the available increase in parameter e_C between a smaller diameter and shorter length, as he desires.

4078

A limiting curve is drawn on part (a) of the charts. Regions above this curve are turboprop designs, and those below, turbojet. Appendix B presents the derivation of this limiting curve.

Point B on chart I(a) shows that for this flight condition the lowest stress at which a turbine can drive compressors with e_C of 44×10^6 pounds per second^3 is 26,600 pounds per square inch. Points on or immediately above the limiting curve, however, represent designs of zero or negligible propeller thrust. This is reflected in terms of high specific fuel consumption. If, for example, a turbine of 30,000-pound-per-square-inch stress is sought to drive a compressor with e_C of 44×10^6 pounds per second^3, chart I(a) shows that the turbine pressure ratio is 4.25 if the compressor pressure ratio is 10. On chart I(b) this point is located at high specific fuel consumption.

Figure 4 shows this latter point most clearly for a turbine-inlet temperature of 2075° R. On figure 4, the curve of constant values of p_2'/p_1' are reproduced from chart I(b). The dotted lines on figure 4 show the values of turbine stress resulting if the turbines are to drive compressors with an e_C of 44×10^6 pounds per second^3. This figure shows the high specific fuel consumption and low hp/A_T resulting if turbine stress is limited to 30,000 pounds per square inch. For e_C of 44×10^6 pounds per second^3, the turbine must operate at a stress of nearly 50,000 pounds per square inch for low specific fuel consumption and highest hp/A_T.

For turbine-inlet temperatures of 2593° R, chart II(b) discloses that, on the basis of lowest specific fuel consumption and highest hp/A_T, optimum compressor pressure ratio becomes approximately 20. To develop such a high compressor pressure ratio in a one-spool engine requires a large number of stages. Therefore, considering what might be achieved in the reasonably near future, the compressor pressure ratio might preferably be selected at values between 10 and 15.

Furthermore, chart II(b) shows little to be gained by increasing the compressor pressure ratio from 15 to 20. The reason for this is that, as compressor pressure ratio rises, the compressor takes up a larger proportion of the turbine work output. In order for engine horsepower per turbine frontal area to show a substantial increase as compressor pressure ratio exceeds 15, the turbine-inlet temperature must be raised above 2593° R. This fact is demonstrated by charts I(b) and II(b). These charts show that the best compressor pressure ratio is 10 at 2075° R; whereas at 2593° R a value of 20 is best.

At a turbine-inlet temperature of 2593° R, any engines in which the value of compressor parameter e_C is 44×10^6 pounds per second^3 and the

turbine operates at a stress of 30,000 pounds per square inch also run at unacceptably high specific fuel consumption and low hp/A_T. This is shown by charts II(a) and (b), for such designs are to be found in the region of choked exhaust nozzles, which for these cases yield poor designs.

Figure 5 was constructed from the information given on chart II to show the effects of compressor and turbine pressure ratios and A_E/A_T on turbine stress. A turbine-inlet temperature of 2593° R and an e_C of 44×10^6 pounds per second^3 were used in making this plot. This figure shows that increasing the compressor pressure ratio with A_E/A_T constant results in lowered turbine stress. On the other hand, increasing the turbine pressure ratio with the compressor pressure ratio held fixed results in raising the stress.

Figure 6, plotted from information given on charts I and II for parameter e_C of 44×10^6 pounds per second^3 and A_E/A_T of 1.0, shows that increasing the turbine-inlet temperature results in higher turbine stress for any given value of compressor pressure ratio.

Information given on chart II was used in plotting figure 7, which shows the variation in e_C with σ_T and p_2'/p_1' for a turbine-inlet temperature of 2593° R. At a constant compressor pressure ratio, e_C varies directly with turbine stress. For a given flight condition, turbine-inlet temperature, and compressor pressure ratio, it can be shown that m_T is constant for either a specified value of p_3'/p_4' or of specific fuel consumption. Equation (B13) then shows that e_C varies directly with σ_T.

The curves of constant stress in figure 7(a) were drawn assuming a constant turbine pressure ratio of 6. These curves were not extended beyond values of the abscissa p_2'/p_1' of 12.5, because both specific fuel consumption and hp/A_T deteriorate above this point for a turbine pressure ratio of 6. This figure shows clearly that, to drive advanced compressors (high e_C), turbines must operate at high stress. For example, the corresponding point for point C on chart II(b) is shown on figure 7(a) at 44×10^6 pounds per second^3. The turbine for this design must operate at a stress of about 47,000 pounds per square inch. It bears repeating that this stress may not be intolerable because of the high turbine pressure ratio and, hence, low turbine-outlet temperature. In any event, a turbine of 30,000-pound-per-square-inch stress cannot drive an advanced compressor without deterioration of specific fuel consumption and hp/A_T.

Figure 7(a) shows that, for a given stress, increasing the compressor pressure ratio permits the turbines to drive compressors of higher e_C. Or, alternatively, increasing the compressor pressure ratio at constant e_C results in lower turbine stress. Chart II(b), however, indicates that increasing the compressor pressure ratio with constant turbine pressure ratio is accompanied by increasing specific fuel consumption.

Increasing compressor pressure ratio need not result in increased specific fuel consumption, as was just seen to occur in figure 7(a) for constant turbine pressure ratio. Figure 7(b) is similar to figure 7(a), but it is plotted for a constant specific fuel consumption of 0.64 pound of fuel per horsepower-hour. This figure, like figure 7(a), shows that parameter e_C rises with increasing p_2'/p_1' for constant σ_T. The specific fuel consumption now, however, is constant. For a stress of 30,000 pounds per square inch, figure 7(b) shows that e_C does not exceed 39×10^6 pounds per second^3. These observations indicate that, if in turboprop-engine design the turbine stress is limited to 30,000 pounds per square inch, it is desirable to strive for high compressor pressure ratio at low values of parameter e_C. This is in contrast with the aim in design of compressors for high Mach number turbojet engines, for in the latter case low compressor pressure ratio is required at high values of e_C.

If, however, turbine stress can be increased in the future, it appears from figure 7(b) that parameter e_C will exceed presently obtainable values. Thus, the primary limitation shifts from turbine stress to compressor aerodynamics.

Sea-Level Designs at Mach 0.6

Charts III and IV show turboprop-engine performance for turbine-inlet temperatures of 1668° and 2225° R, respectively, for Mach 0.6 designs at sea level. On chart III(b), where the turbine-inlet temperature is 1668° R, the compressor pressure ratio for lowest specific fuel consumption is 7. If T_3' is raised to 2225° R (chart IV(b)) the best value of p_2'/p_1' is about 15. The value of A_E/A_T for lowest specific fuel consumption is between 0.8 and 0.85 on both charts III(b) and IV(b).

To drive a compressor having a value for e_C of 44×10^6 pounds per second^3, a turbine with an inlet temperature of 1668° R must run at a stress of at least 37,000 pounds per square inch (chart III(a)) and preferably over 50,000 pounds per square inch in order to obtain low specific fuel consumption. Chart IV(a) shows that it is possible for turbines of

4078
CU-2

30,000-pound-per-square-inch stress to drive compressors of 44×10^6 pounds per second^3. Such designs are so close to the limiting curve that they would surely suffer because of high specific fuel consumption, for the reasons mentioned earlier.

Figure 8 is taken from information given on chart IV(b). The curves of constant stress are drawn for a value of e_C of 44×10^6 pounds per second^3. This plot shows that turbines designed to operate at a stress of 30,000 pounds per square inch can drive compressors with an e_C of 44×10^6 pounds per second^3 only at high values of specific fuel consumption. Figure 8 further shows that, for a given value of specific fuel consumption, higher values of hp/A_T are obtained as turbine stress is decreased, but p_2'/p_1' must be increased in so doing. Or, for a constant p_2'/p_1', higher hp/A_T is obtained as turbine stress is decreased, but at the expense of raising specific fuel consumption.

4078

This last circumstance can be illustrated by considering points D and E on the curve for a compressor pressure ratio of 10. Point D is for a stress of 50,000 pounds per square inch, and point E is for a stress of 40,000 pounds per square inch. By reading the values of m_T for these two cases on chart IV(a), the resultant engine power per unit weight flow is $12\frac{1}{2}$ percent lower for the turbine of 40,000 pounds per square inch. Furthermore, the frontal area per unit weight flow of the lower-stress turbine is 21 percent lower. This greater decrease in area per unit weight flow offsets the decrease in power per unit weight flow, which results in higher hp/A_T at 40,000 pounds per square inch. The smaller frontal area per unit weight flow, with e_C constant, results in lower stress. Also, since the engine power per unit weight flow is reduced by a less favorable split between propeller and jet thrust for the 40,000-pound-per-square-inch case, the specific fuel consumption increases since the ratio of the fuel flow to weight flow is constant.

On figure 9, plotted from information given on chart IV(a), the variation in turbine stress with compressor and turbine pressure ratios and with A_E/A_T is shown. On this plot, the turbine-inlet temperature is 2225° R and parameter e_C is 44×10^6 pounds per second^3. For a constant value of A_E/A_T, increasing p_2'/p_1' results in lower σ_T, just as was observed in the sea-level static designs. This figure also shows that, for a given value of p_2'/p_1', increasing p_3'/p_4' results in increasing stress. It will be noticed that the ratio A_E/A_T rises for such a case. Alternatively, increasing p_3'/p_4' at constant A_E/A_T yields lower stress, as p_2'/p_1' also increases.

Figure 10 was plotted from data given on charts III(a) and IV(a) with e_C of 44×10^6 pounds per second^3 and A_E/A_T of 0.8. This plot shows that increasing the turbine-inlet temperature results in increased turbine stress.

Tropopause Designs at Mach 0.6

For turbine-inlet temperatures of 1672°, 2090°, and 2509° R, respectively, charts V, VI, and VII present turboprop-engine performance for Mach 0.6 designs at the tropopause. For a turbine-inlet temperature of 1672° R, chart V(b) shows that a compressor pressure ratio of 12 yields the lowest specific fuel consumption. At temperatures of 2090° and 2509° R, charts VI(b) and VII(b) indicate theoretically best values of compressor pressure ratio of 25 and 40, respectively. Such high values are of academic interest, only, and are shown merely for completeness. At T_3' of 1672° R, a value for A_E/A_T of about 0.72 yields lowest specific fuel consumption. For inlet temperatures of 2090° and 2509° R, a value of 1.0 for A_E/A_T results in lowest specific fuel consumption.

Figure 11 has been drawn for a turbine-inlet temperature of 2090° R (data from chart VI) and is similar to figures 4 and 8. Again, although turbines designed for a 30,000-pound-per-square-inch stress yield higher hp/A_T for a given p_2'/p_1' than those of 40,000-pound-per-square-inch stress, the resultant horsepower per unit weight flow is less. And, in turn, the horsepower per unit weight flow is less for turbines designed for a stress of 40,000 pounds per square inch than those designed for 50,000 pounds per square inch. Nevertheless, figure 11 shows that a wider range of turbine designs for a stress of 30,000 pounds per square inch is possible than for the sea-level flight conditions (fig. 8). This implies that the stress problem is less severe for flight at a Mach number of 0.6 at the tropopause than at sea level. At a compressor pressure ratio of 15, specific fuel consumption can be reduced from a value of 0.467 to 0.405 pound fuel per horsepower-hour if stress is increased from 30,000 to 50,000 pounds per square inch.

In figure 12, which was derived from chart VI(a), turbine stress is plotted against turbine pressure ratio for curves of constant p_2'/p_1' and of constant A_E/A_T. For this plot, the turbine-inlet temperature is 2090° R and the parameter e_C is 44×10^6 pounds per second^3. Once again it is found that increasing the compressor pressure ratio yields lower stress. This is true if either A_E/A_T or p_3'/p_4' is held constant.

For a value of 44×10^6 pounds per second^3 for parameter e_C and for A_E/A_T of 0.75, turbine stress is plotted against turbine-inlet temperature for three selected values of compressor pressure ratio in figure 13.

4078

CU-2 back

The data for this plot were read from charts V(a), VI(a), and VII(a). In engine designs made for flight at a Mach number of 0.6 at the tropopause, increasing the turbine-inlet temperature results in increasing turbine stress.

Figure 14 is a plot of parameter e_C against p_2'/p_1' with curves of constant specific fuel consumption. This figure was constructed from chart VI for a turbine-inlet temperature of 2090° R and a turbine stress of 30,000 pounds per square inch. First of all, this figure reveals, as did the designs for the sea-level static condition, that increasing the compressor pressure ratio makes a turbine of a given stress capable of driving compressors of high parameter e_C. This figure further discloses that low values of specific fuel consumption and high values of e_C are unobtainable for this flight condition and temperature in an engine with 30,000-pound-per-square-inch stress in the turbine without going to high p_2'/p_1'. For example, for a specific fuel consumption of 0.45 pound fuel per horsepower-hour, a turbine designed to operate at 30,000-pound-per-square-inch stress cannot drive a compressor of e_C of 44×10^6 pounds per second^3 unless the design value of compressor pressure ratio is about 18.

If a turbine stress of 40,000 pounds per square inch can be tolerated, a design can be made in which specific fuel consumption and e_C remain at 0.45 pound per horsepower-hour and 44×10^6 pounds per second^3, respectively, and p_2'/p_1' is reduced to a value of 12. This design is designated as point F on chart VI. On the other hand, if σ_T is fixed at 30,000 pounds per square inch and e_C at 44×10^6 pounds per second^3, the resulting value of specific fuel consumption is 0.505 pound per horsepower-hour if p_2'/p_1' is 12 (point G on chart VI and fig. 14). From this it can be concluded that, if turbine stress must be limited to 30,000 pounds per square inch and compressor pressure ratio to 12, the turbine can drive a compressor with e_C of 44×10^6 pounds per second^3, but the engine suffers by increased specific fuel consumption.

Tropopause Designs at Mach 0.8

Tropopause designs at 0.8 Mach number are presented in charts VIII, IX, X, and XI for turbine-inlet temperatures of 1750°, 2200°, 2641°, and 3000° R, respectively. On chart VIII(b) it can be seen that the compressor pressure ratio for lowest specific fuel consumption for T_3' of 1760° R is about 15. At T_3' of 2200° R (chart IX(b)), a compressor pressure

ratio of 25 yields the lowest specific fuel consumption. At higher temperatures (2641° and 3000° R, charts X(b) and XI(b)), the compressor pressure ratio for lowest specific fuel consumption is much higher.

With regard to the ratio A_E/A_T, chart VIII(b) indicates that a value of about 0.72 yields lowest specific fuel consumption. At T_3' of 2200°, 2641°, and 3000° R, the corresponding values of A_E/A_T are about 0.75, 0.72, and 0.705. At a turbine-inlet temperature of 3000° R, values of A_E/A_T greater than 0.705 are not shown, because, as chart XI(a) shows, the resulting turbine stresses become very high for values of e_C as low as even 30×10^6 pounds per second^3.

4078

Figure 15 was plotted for a turbine-inlet temperature of 2200° R, and the data were taken from chart IX(b). Parameter e_C is held constant at 44×10^6 pounds per second^3 in this figure. At a compressor pressure ratio of 15, this figure shows that specific fuel consumption can be reduced 9 percent by increasing the turbine stress from 30,000 to 40,000 pounds per square inch. An additional 3-percent decrease in specific fuel consumption is possible if the turbine stress is further increased to 50,000 pounds per square inch.

At a turbine-inlet temperature of 2641° R, figure 16 shows that for this flight condition, just as for the others considered herein, increasing compressor pressure ratio results in decreasing turbine stress when e_C and A_E/A_T are held constant. At p_2'/p_1' of 15, the exhaust nozzle must be choked for stresses below 49,000 pounds per square inch to be considered.

The variation in turbine stress with turbine-inlet temperature for this flight condition is presented in figure 17. This figure shows that turbine stress increases with increasing turbine-inlet temperature. This has also been found to be true in the other flight conditions studied.

Comparisons

In figure 4, it is seen that, if the turbine stress is 30,000 pounds per square inch when e_C is 44×10^6 pounds per second^3, the specific fuel consumption is very high for all designs. In figure 8, only one design of a turbine with a stress of 30,000 pounds per square inch is shown, and this design results in high specific fuel consumption. Thus, if turbine stress is limited to 30,000 pounds per square inch, turbines designed for the sea-level condition can drive compressors of parameter e_C of 44×10^6 pounds per second^3, but the resulting specific fuel consumption is unacceptably high. Figures 11 and 15, drawn for design conditions at the

tropopause, show that, if turbine stress is 30,000 pounds per square inch and e_C is 44×10^6 pounds per second^3, the resulting specific fuel consumption is considerably improved in value over the sea-level designs. This suggests that turbine stress is a more serious problem for sea-level designs than for subsonic designs at the tropopause. This contention is corroborated by figure 18, in which stress is plotted against turbine-inlet temperature with curves of constant engine temperature ratio for the various flight conditions considered. Assumed in this figure are p_2'/p_1' of 10, p_3'/p_4' of 6, and e_C of 44×10^6 pounds per second^3. These curves indicate that the most severe stress problem is for sea-level flight at a Mach number of 0.6, while sea-level static designs are somewhat less severe. The stress problem is less serious for subsonic flight at the tropopause, the stresses at a Mach number of 0.6 being lower than those at a Mach number of 0.8. These results can be explained by consideration of equation (B12). In this equation $(\rho V_x/\rho' a_{cr}')_4$ is constant. Since p_2'/p_1' and p_3'/p_4' are held fixed in making the cross plot, all other factors on the right side in equation (B12) are constant except T_3'/T_1' and f. In the calculations, f was calculated for each point, but little variance was found. Therefore, along the lines of constant engine temperature ratio, there is approximately a linear variation of σ_T with θ_1', because e_C is constant. The following table lists θ_1' for the four flight conditions:

M_0	Altitude	θ_1'
0	Sea level	1
.6	Sea level	1.072
.6	Tropopause	.806
.8	Tropopause	.848

It is seen from this table, then, that the observed variations of turbine stress with flight conditions arise from variations of the value of θ_1'.

It can also be observed that under the assumptions used in plotting figure 18 an increase in turbine-inlet temperature is accompanied by a stress increase.

In figure 19 the effects on turbine stress of varying the ratio of exhaust-nozzle to turbine frontal area and flight Mach number are shown. On this plot $e_C = 44\times10^6$ pounds per second^3 and $p_2'/p_1' = 10$. At sea level, an engine temperature ratio of 4 is maintained on the plot; for the tropopause designs, the curves are drawn for a value of T_3'/T_1' of 5. Thus, for this figure, the turbine-inlet temperature is about 2100° to 2200° R.

4078

These curves show clearly, for all flight conditions investigated, the advantages in stress reduction afforded by reducing the ratio A_E/A_T. The lowest stress is obtained at a value of 0.705, at which point the exhaust nozzle chokes. Of course, specific fuel consumption rises with reduction in A_E/A_T, as shown on the charts.

For any given value of A_E/A_T and the same engine temperature ratio, increasing the flight Mach number results in stress increases at both altitudes considered.

4078

CONCLUSIONS

The following conclusions have been drawn from this design-point analysis of one-spool turboprop engines:

1. Turbine centrifugal stress is a primary limitation for all flight conditions considered.

2. Increasing the compressor pressure ratio relieves the turbine stress and reduces the specific fuel consumption. It appears desirable to strive for high compressor pressure ratio at low tip speeds and low weight flows per unit frontal area. This is in contrast with the aim in high Mach number turbojet design, for in the latter case high tip speeds and high weight flows per unit frontal area are required at low compressor pressure ratios.

3. The problem of turbine centrifugal stress is more severe for sea-level design conditions than for design conditions of subsonic flight at the tropopause.

4. For most sea-level designs, turbines operating at a stress of 30,000 pounds per square inch are capable of driving compressors of high weight flow per frontal area and high tip speed. They do so, however, only at high specific fuel consumption. Furthermore, many such designs represent negligible propeller thrust.

5. Increasing turbine-inlet temperature is accompanied by increasing turbine centrifugal stress.

6. If turbine stresses above 50,000 pounds per square inch can by some means be tolerated, the primary limitation might shift to the compressor, for compressor aerodynamics becomes a severe problem.

7. For sea-level static designs, lowest specific fuel consumption can be obtained if the turbine frontal area is about the same size as the exhaust nozzle. This is also true of flight at a Mach number of 0.6 at

the tropopause for turbine-inlet temperatures of 2090° R and higher. Values between 0.75 and 0.85 for the ratio of exhaust-nozzle to turbine frontal area yield lowest specific fuel consumption for a Mach number of 0.6 at sea level and a Mach number of 0.8 at the tropopause for turbine-inlet temperatures up to 2641° R.

8. In engines designed for a Mach number of 0.8 at the tropopause with a turbine-inlet temperature of 3000° R, the exhaust nozzle should be choked in order to avoid excessive values of turbine centrifugal stress.

9. Reduction in the ratio of exhaust-nozzle to turbine frontal area results in reduced turbine stress.

Lewis Flight Propulsion Laboratory
National Advisory Committee for Aeronautics
Cleveland, Ohio, September 7, 1956

4078

APPENDIX A

SYMBOLS

A	frontal area, sq ft
a	sonic velocity, $\sqrt{\gamma gRT}$, ft/sec
a'_{cr}	critical velocity, $\sqrt{\frac{2k}{k+1} gRT'}$, ft/sec
b	fraction of weight flow bled from compressor
C_n	exhaust-nozzle velocity coefficient
c	equivalent tip speed, $U_t/\sqrt{\theta'_1}$, ft/sec
e	engine parameter used in relating compressors and turbines, mc^2, lb/sec^3
f	fuel-air ratio, lb fuel/lb air
g	constant of gravity
H	lower heating value of fuel at 600° R, Btu/lb fuel
h	specific enthalpy, Btu/lb
h_f	initial enthalpy of fuel, Btu/lb fuel
hp	engine horsepower, hp
J	mechanical equivalent of heat
k	ratio of specific heats for gas at exhaust-nozzle exit
M	Mach number relative to rotating blades
m	equivalent weight flow per unit frontal area, $\frac{w\sqrt{\theta'_1}}{A\delta'_1}$, (lb/sec)/sq ft
p	absolute pressure, lb/sq ft
R	gas constant

4078

CU-3

r radius, ft

sfc specific fuel consumption, lb fuel/hp-hr

T absolute temperature, $^{\circ}R$

U blade velocity, ft/sec

V absolute velocity, ft/sec

w weight flow, lb/sec

Γ density of blade metal, lb/cu ft

γ ratio of specific heats for air in free stream

δ ratio of pressure to NACA standard sea-level pressure, p/2116

η_B burner efficiency

η_G gearbox efficiency

η_P propeller efficiency

η_∞ small-stage efficiency

θ ratio of temperature to NACA standard sea-level temperature, T/518.7

λ stress-correction factor for tapered blades

ρ density of gas, lb/cu ft

σ blade centrifugal stress at hub radius, psi

ψ_h $\dfrac{(h - h_a)(1 + f)}{f}$, Btu/lb

ω angular velocity, radians/sec

Subscripts:

a air

C compressor

4078

E exhaust nozzle

h hub

j jet

T turbine

t tip

x axial component

0 free stream

1 compressor inlet

2 compressor outlet

3 turbine inlet

4 turbine outlet

5 exhaust-nozzle outlet

6 station outside exhaust nozzle

Superscript:

' stagnation state relative to stator

4078

CU-3 back

APPENDIX B

ANALYSIS AND CONSTRUCTION OF CHARTS

Analysis

In this analysis, values must be assumed for many design variables. The following parameters and assumed values are used in the present analysis:

4078

$\left(\frac{\rho V_x}{\rho' a'_{cr}}\right)_4$	0.562
$p'_1/p'_0 = p'_3/p'_2 = p'_5/p'_4$	0.95
$(r_h/r_t)_4$	0.5
$\eta_{\infty,T}$	0.85
$\eta_{\infty,C}$	0.88
η_B	0.95
η_G	0.95
η_P	0.80
H, Btu/lb fuel	18,574
h_f, Btu/lb fuel	-50
Γ, lb/cu ft	500
λ	0.7
C_n	0.96
$(r_h/r_t)_1$	0.4
b	0
g, ft/sec^2	32.2
J, ft-lb/Btu	778.2
R, ft-lb/(lb)($^{\circ}$R)	53.4

Cycle analysis. - The calculation procedure was begun by first assuming a range of values for the compressor pressure ratio p'_2/p'_1 while simultaneously varying the turbine pressure ratio p'_3/p'_4. Compressor pressure ratios from 2 to 40 were assumed in equal increments of the natural logarithm. The ratio p'_4/p'_1 was maintained within the limits

$$0.8 \leq \frac{p'_4}{p'_1} \leq \frac{p'_3}{p'_2}\,\frac{p'_2}{p'_1}\left\{1 - \frac{\gamma}{\gamma - 1}\,\frac{k - 1}{k}\,\frac{\left[\left(\frac{p'_2}{p'_1}\right)^{\frac{\gamma - 1}{\gamma\eta_{\infty,C}}} - 1\right]}{\frac{T'_3}{T'_1}}\right\}^{\frac{k}{k-1}\,\frac{1}{\eta_{\infty,T}}} \tag{B1}$$

where the upper limit is the value for a turbojet engine if it is assumed that $w_T = w_C$.

The turbine pressure ratio p_3'/p_4' is used to determine the turbine-outlet stagnation temperature T_4' by means of the method described in reference 2. However, the fuel-air ratio f must be evaluated first. Reference 2 gives as a formula for f:

$$f = \frac{h_{a,3} - h_{a,2}}{\eta_B H - h_{a,3} - \psi_{h,3} + h_f} \tag{B2}$$

The parameter $h_{a,2}$ is obtained by using the method of reference 2 along with the compressor pressure ratio p_2'/p_1' and small-stage efficiency $\eta_{\infty,C}$. The parameters $h_{a,3}$ and $\psi_{h,3}$ are also obtained by the method of reference 2 by using the assigned turbine-inlet temperature T_3'. A value for each of the constants η_B, H, and h_f is given on the preceding page.

Turbine-limited specific weight flow m_T is calculated from

$$m_T = \frac{w_T\sqrt{\theta_1'}}{A_T\delta_1'} = \frac{2116}{\sqrt{518.7}}\sqrt{\frac{2kg}{(k+1)R}}\left(\frac{\rho V_x}{\rho' a_{cr}'}\right)_4\left[1 - \left(\frac{r_h}{r_t}\right)_4^2\right]\frac{\frac{p_4'}{p_1'}}{\sqrt{\frac{T_4'}{T_3'}\frac{T_3'}{T_1'}}} \tag{B3}$$

where the ratio p_4'/p_1' is calculated as follows:

$$\frac{p_4'}{p_1'} = \frac{p_2'}{p_1'}\frac{p_4'}{p_3'}\frac{p_3'}{p_2'} \tag{B4}$$

The method of reference 2 is used to calculate the specific enthalpy changes across the compressor $\Delta h_C'$ and across the turbine $\Delta h_T'$ from their known pressure ratios.

The exhaust-nozzle pressure ratio is found from

$$\frac{p_6}{p_5'} = \left(\frac{p}{p'}\right)_0 \frac{p_0'}{p_1'}\frac{p_1'}{p_2'}\frac{p_2'}{p_3'}\frac{p_3'}{p_4'}\frac{p_4'}{p_5'} \tag{B5}$$

since it is assumed that

$$p_0 = p_6$$

Equation (B5) is then used in calculating the jet velocity:

$$V_j = C_n \sqrt{\frac{2k}{k - 1} gRT_4' \left[1 - \left(\frac{p_6}{p_5'}\right)^{\frac{k-1}{k}}\right]} \tag{B6}$$

The flight velocity is

$$V_0 = \sqrt{\gamma gRT_0}\, M_0 \tag{B7}$$

and the turbine weight flow per unit turbine frontal area is

$$\frac{w_T}{A_T} = m_T \left(\frac{p_1'}{p_0'}\right)\left(\frac{p_0'}{p_0}\right)\left(\frac{p_6}{2116}\right)\sqrt{\frac{518.7}{T_0}}\sqrt{\left(\frac{T_0}{T_0'}\right)} \tag{B8}$$

For engines having their design points at the sea-level static conditions, engine horsepower per unit turbine frontal area is

$$\frac{hp}{A_T} = \frac{w_T}{A_T}\left[\frac{J\eta_G}{550}\left(\Delta h_T' - \frac{\Delta h_C'}{1 + f}\right) + \frac{V_j}{2.5g}\right] \tag{B9}$$

The constant 2.5 is an arbitrary value used to convert static thrust to horsepower. Specific fuel consumption is calculated from

$$sfc = \frac{3600\ f}{\frac{hp/A_T}{w_T/A_T}(1 + f)} \tag{B10}$$

For engines having their design point at Mach numbers other than zero, specific engine horsepower is calculated from

$$\frac{hp}{A_T} = \frac{w_T/A_T}{550}\left[J\eta_G\left(\Delta h_T' - \frac{\Delta h_C'}{1 + f}\right) + \frac{V_0\left(V_j - \frac{V_0}{1 + f}\right)}{g\eta_P}\right] \tag{B11}$$

and specific fuel consumption from equation (B10).

The number of turbine stages required is not investigated in this analysis. This information can be obtained from reference 3. With the turbines designed for limiting loading [i.e., $(\rho V_x/p'a'_{cr})_4 = 0.562$], the smallest exit annular area is obtained for a given work output. The same work output, of course, is obtainable from a turbine designed below the point of limiting loading, but its exit annular area would be larger.

In this analysis, no allowance has been made for the effects on turbine weight flow and work output that would result from turbine cooling. Cooling of the turbine blades would be required in many of the designs studied in this report, since turbine-inlet temperatures as high as 3000° R are considered.

Turbine blade centrifugal stress. - The compressor parameter e_C and the turbine blade centrifugal stress at the hub radius of the last rotor are related from

$$\frac{\sigma_T/\theta'_1}{e_C} = \frac{\Gamma\lambda}{288}\,\frac{\sqrt{518.7}}{2116}\sqrt{\frac{(k+1)R}{2kg^3}}\,(1+f)\,\frac{(1-b)}{\left(\frac{\rho V_x}{p'a'_{cr}}\right)_4}\,\frac{\sqrt{\frac{T'_4}{T'_3}\,\frac{T'_3}{T'_1}}}{\frac{p'_4}{p'_1}} \tag{B12}$$

Combining equations (B3) and (B12) by eliminating $\frac{p'_4}{p'_1}\sqrt{\frac{T'_1}{T'_4}}$ yields

$$\frac{\sigma_T/\theta'_1}{e_C} = \frac{\Gamma\lambda}{288}\,\frac{(1+f)(1-b)}{gm_T}\left[1-\left(\frac{r_h}{r_t}\right)_4^2\right] \tag{B13}$$

Parameter e. - Since parameter e is defined as

$$e = mc^2$$

then

$$\left.\begin{aligned} e_C &= \frac{w_C U_{t,C}^2}{A_C\delta'_1\sqrt{\theta'_1}} = \frac{w_C\omega^2}{\pi\delta'_1\sqrt{\theta'_1}} \\ e_T &= \frac{w_T U_{t,T}^2}{A_T\delta'_1\sqrt{\theta'_1}} = \frac{w_T\omega^2}{\pi\delta'_1\sqrt{\theta'_1}} \end{aligned}\right\} \tag{B14}$$

Because compressor and turbine weight flows bear the relation

$$w_T = (1 + f)(1 - b)w_C$$

parameters e for compressors and turbines are related by

$$e_T = (1 + f)(1 - b)e_C \tag{B15}$$

Figures 2 and 3 are reproduced from reference 1. These figures illustrate the role that parameter e_C plays in compressor aerodynamics. In figure 2, compressor parameter e_C is plotted against compressor equivalent blade tip speed c_C for various values of compressor rotor inlet relative Mach number M_1. The dotted line is the locus of minimum values of compressor rotor inlet relative Mach number M_1 for given values of parameter e_C. The additional abscissa scale is convenient for determining compressor centrifugal stress. In the plotting of figures 2 and 3, it was assumed that the compressors have no inlet guide vanes. A compressor hub-tip radius ratio of 0.4 is assumed in these two figures.

Figure 3 relates compressor parameters for maximized parameter e_C, that is, points on the dotted line of figure 2. Maximized parameter e_C and equivalent specific air flow m_C are plotted against compressor rotor inlet relative Mach number M_1 in figure 3(a). Compressor equivalent blade tip speed c_C and compressor-inlet absolute Mach number $(V/a)_1$ are plotted against M_1 in figure 3(b).

Turbine aerodynamics. - It is stated earlier that all turbines in this analysis are designed at the limiting-loading condition. Throughout the analysis a value of 0.562 is assumed for turbine-exit specific weight-flow parameter $(\rho V_x/\rho' a'_{cr})_4$. This value is obtained at a turbine-exit axial Mach number of 0.7 and zero exit whirl.

Turbine-limited specific weight flow m_T is calculated from equation (B3). Throughout this analysis a constant value of 0.5 was assumed for the turbine hub-tip radius ratio $(r_h/r_t)_4$ at the rotor exit.

Engine geometry. - In order to relate engine geometry with engine operating parameters, the ratio of exhaust-nozzle to turbine frontal area is calculated from

$$\frac{A_E}{A_T} = \frac{(\rho V_x/\rho' a'_{cr})_4}{(\rho V_x/\rho' a'_{cr})_5}\left[1 - \left(\frac{r_h}{r_t}\right)_4^2\right]\frac{p'_4}{p'_5} \tag{B16}$$

For the case of a choking exhaust nozzle, when $\left(\frac{p_6}{p_5'}\right) \leq \left(\frac{2}{k+1}\right)^{\frac{k}{k-1}}$,

$$\left(\frac{\rho V_x}{\rho' a_{cr}'}\right)_5 = \left(\frac{2}{k+1}\right)^{\frac{1}{k-1}} \tag{B17}$$

and

$$\frac{A_E}{A_T} = 0.705$$

if $k_5 = 4/3$.

For the case of subsonic flow in the exhaust nozzle, when $\left(\frac{p_6}{p_5'}\right) \geq \left(\frac{2}{k+1}\right)^{\frac{k}{k-1}}$,

$$\left(\frac{\rho V_x}{\rho' a_{cr}'}\right)_5 = \left(\frac{p_6}{p_5'}\right)^{\frac{1}{k}} \sqrt{\frac{k+1}{k-1}\left[1 - \left(\frac{p_6}{p_5'}\right)^{\frac{k-1}{k}}\right]} \tag{B18}$$

Construction of Charts

Table I summarizes the flight conditions and engine temperature ratios presented in the charts. The following procedure pertains to each flight condition and turbine-inlet temperature investigated. The left side of parts (a) of the charts consists simply of straight lines which go through the origin (although not shown) and with $\sigma_T/\theta_1' e_C$ plotted against σ_T. The right side of parts (a) of the charts is plotted directly from calculated data of $\sigma_T/\theta_1' e_C$ against p_2'/p_1' with curves of constant turbine stagnation pressure ratio p_3'/p_4'. The ratio p_4'/p_1' used in the calculation of $\sigma_T/\theta_1' e_C$ from equation (B12) was limited as shown in equation (B1).

On the right side of parts (a) of the charts, the dashed lines showing values of constant m_T were obtained by using the calculated values of p_4'/p_1' in equation (B3) and cross-plotting the calculated data.

The dotted lines on the right side of parts (a) of the charts show values of constant ratio of exhaust-nozzle to turbine frontal area A_E/A_T. These curves were obtained by calculating $\sigma_T/\theta_1' e_C$, as before, p_6/p_5' from equation (B5) for the values of p_2'/p_1' and p_3'/p_4', and A_E/A_T from equation (B16). From these calculations, A_E/A_T was plotted against $\sigma_T/\theta_1' e_C$ with constant curves of p_2'/p_1'. Cross-plotting then yielded the dotted curves of constant A_E/A_T on the right side of parts (a) of the charts.

From calculated data, engine horsepower was plotted against compressor pressure ratio for constant values of p_3'/p_4'. Similarly, specific fuel consumption was plotted against compressor pressure ratio. These two preliminary plots were then read at selected values of compressor pressure ratio to produce the curves of constant compressor and turbine pressure ratios shown on the (b) portions of the charts. These curves are independent of turbine stress.

The dotted curves on the (b) portions of the charts show constant values of A_E/A_T. They were obtained from the corresponding dotted lines on parts (a) with the help of either of the preliminary plots just described. As discussed earlier, these curves of constant A_E/A_T are independent of turbine stress. Since the turbine hub-tip radius ratio has been assumed to be 0.5 throughout this analysis, a value of 0.75 for A_E/A_T means that the turbine-exit annular area has the same magnitude as the exhaust-nozzle area. Chart XI(b) has a dotted curve of A_E/A_T of 0.705 only. This means that the exhaust nozzles of all engines on this plot are choked.

On the right side of all the (a) portions of the charts there is drawn a limiting curve. This curve separates turboprop-engine designs from turbojet-engine designs and was determined by the upper limit in equation (B1), where it is assumed that

$$w_C \, \Delta h_C' = w_T \, \Delta h_T'$$

Regions above the limiting curve are turboprop designs, and those below, turbojet. Immediately above the limiting curve, the turboprop-engine design would have practically no propeller thrust. Therefore, such designs cannot be seriously considered as representing true turboprop engines.

REFERENCES

1. Cavicchi, Richard H., and English, Robert E.: Analysis of Limitations Imposed on One-Spool Turbojet-Engine Designs by Compressors and Turbines at Flight Mach Numbers of 0, 2.0, and 2.8. NACA RM E54F21a, 1954.

2. English, Robert E., and Wachtl, William W.: Charts of Thermodynamic Properties of Air and Combustion Products from 3000° to 3500° R. NACA TN 2071, 1950.

3. Cavicchi, Richard H., and English, Robert E.: A Rapid Method for Use in Design of Turbines within Specified Aerodynamic Limits. NACA TN 2905, 1953.

4078

CU-4 back

4078

TABLE I. - SUMMARY OF FLIGHT CONDITIONS AND

ENGINE TEMPERATURES PRESENTED IN CHARTS

Charts	Flight Mach number, M_0	Altitude, ft	Flight velocity		Engine temperature ratio, T_3'/T_1'	Turbine-inlet temperature, T_3', °R
			mph	knots		
I	0	Sea level	0	0	4	2075
II	0	↓	0	0	5	2593
III	.6	↓	456	396	3	1668
IV	.6	↓	456	396	4	2225
V	.6	36,089	396	344	4	1672
VI	.6	↓	396	344	5	2090
VII	.6	↓	396	344	6	2509
VIII	.8	↓	528	458	4	1760
IX	.8	↓	528	458	5	2200
X	.8	↓	528	458	6	2641
XI	.8	↓	528	458	6.82	3000

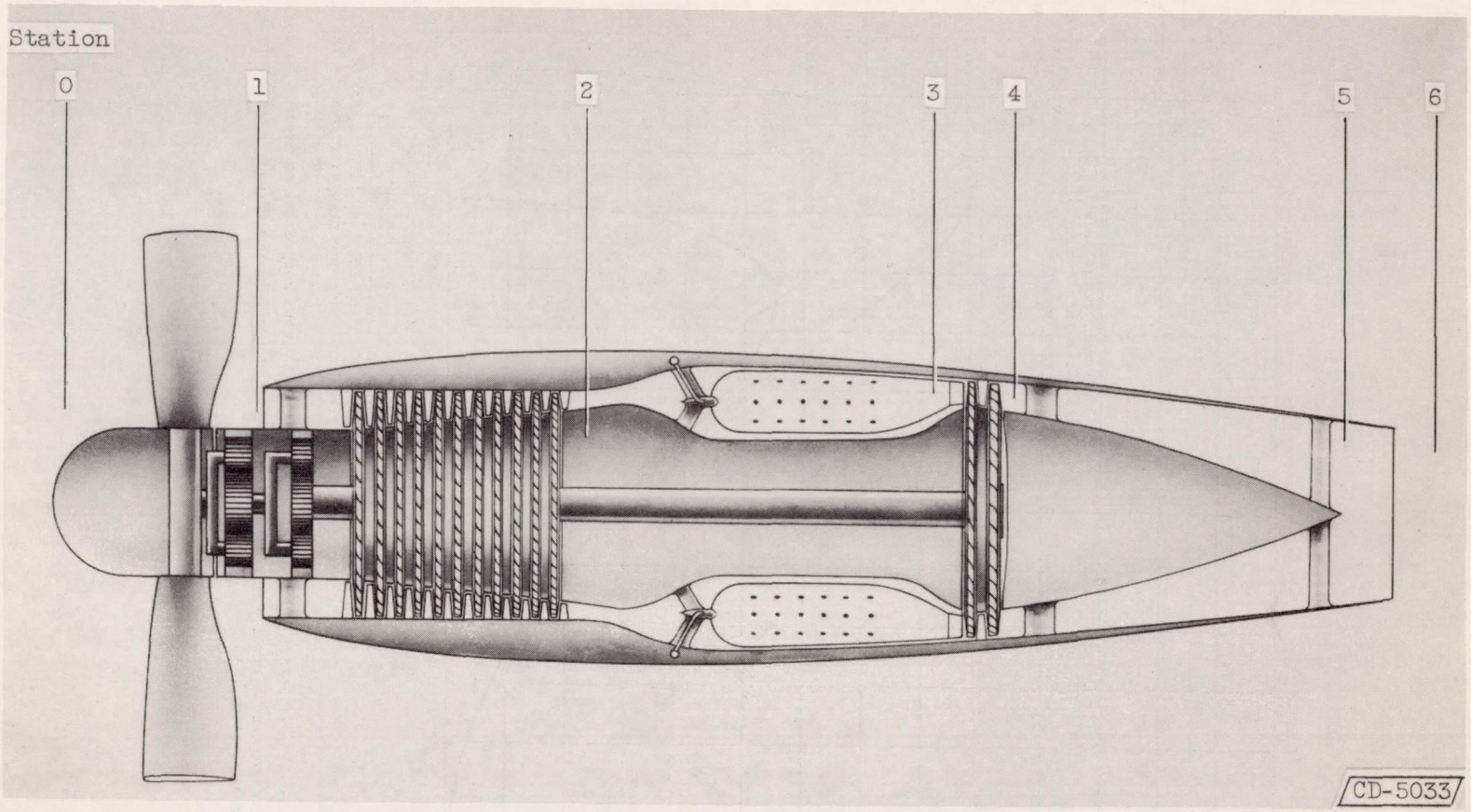

Figure 1. - Schematic sketch of turboprop engine.

4078

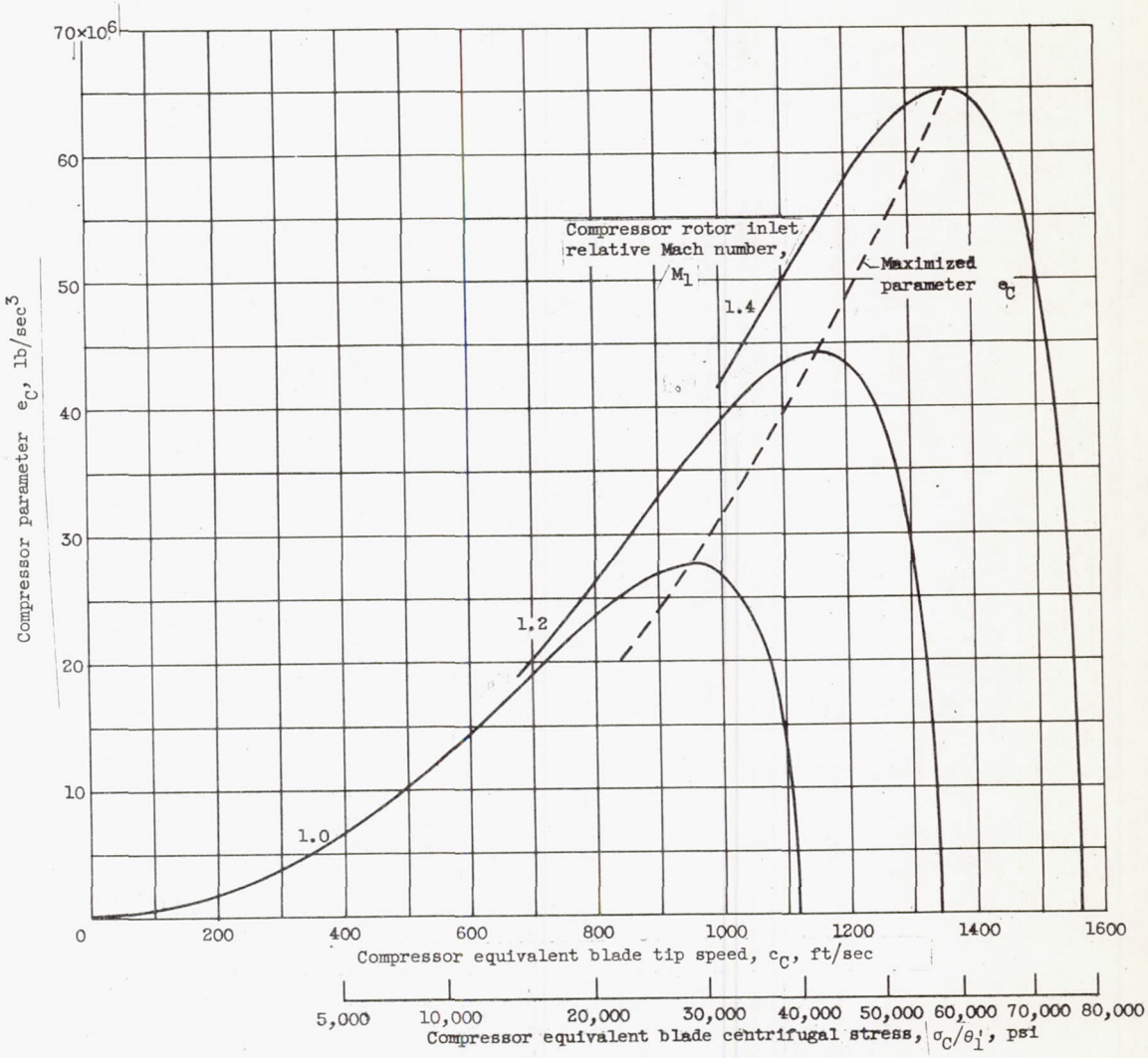

Figure 2. - Variation in compressor parameter e_c with compressor equivalent blade tip speed and compressor rotor inlet relative Mach number (ref. 1, fig. 2(a)). Compressor hub-tip radius ratio, 0.4.

4078

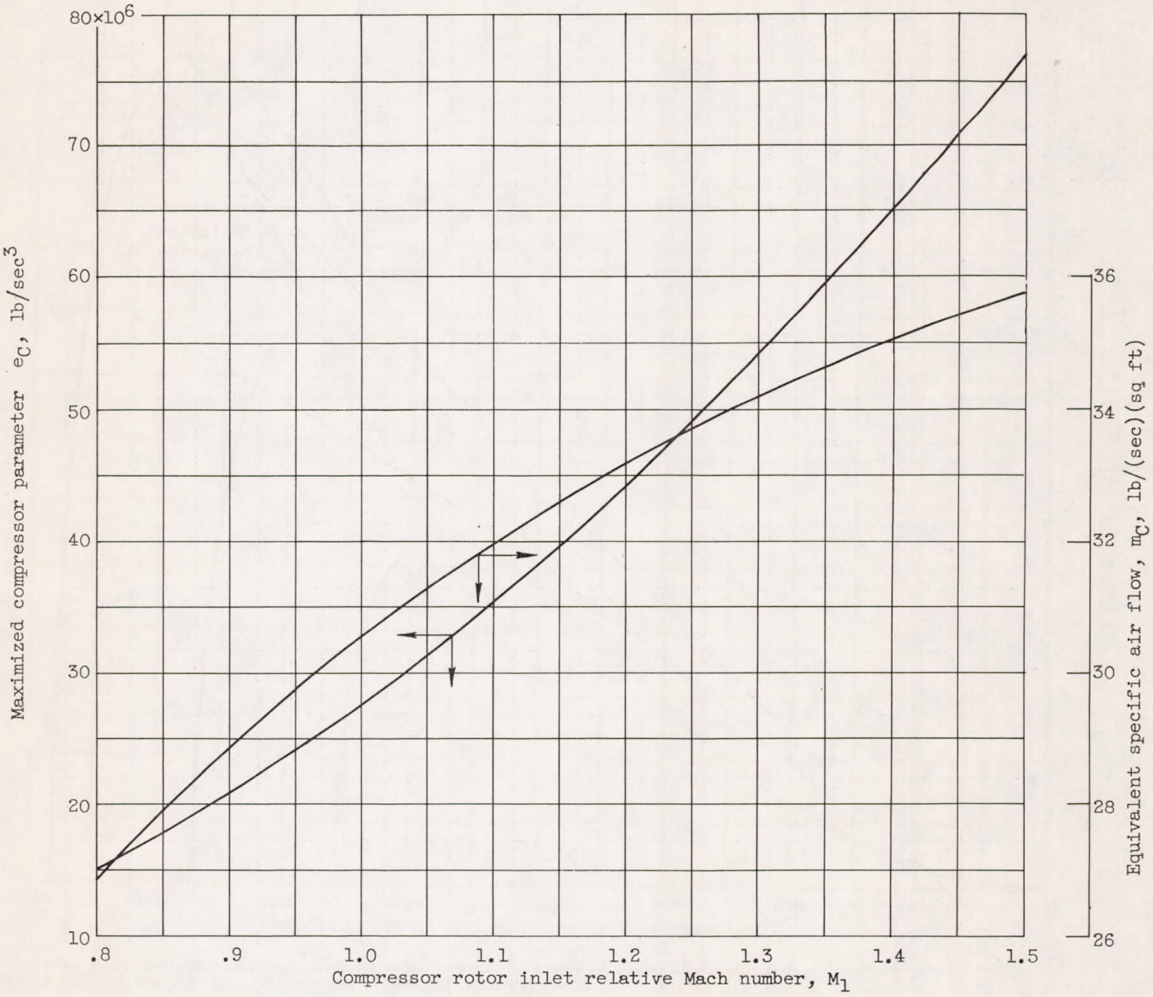

(a) Variation in compressor parameter e_C and specific air flow with compressor rotor inlet relative Mach number (ref. 1, fig. 3(a)); compressor hub-tip radius ratio, 0.4.

Figure 3. - Compressor plots for maximized compressor parameter e_C.

4078

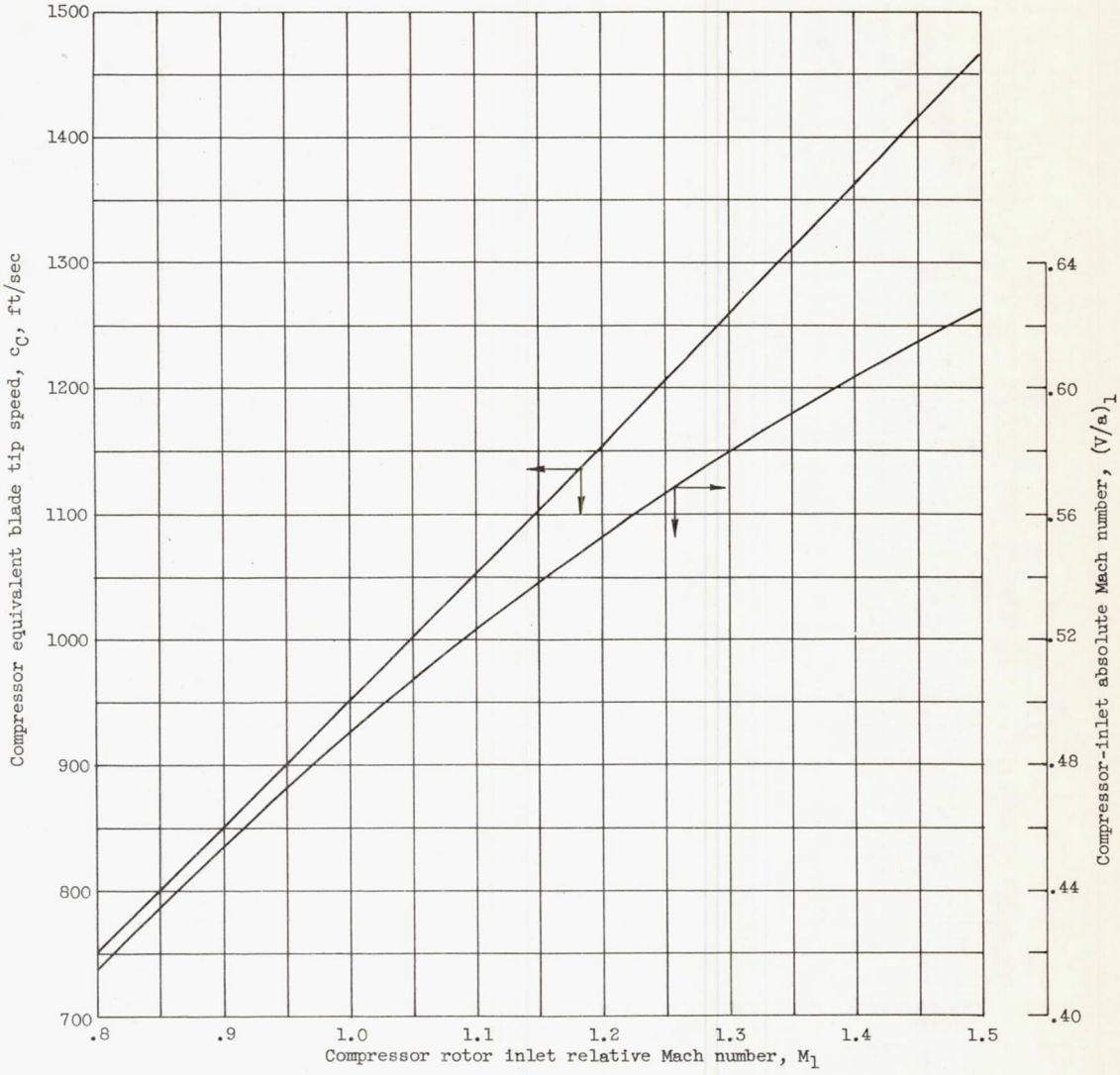

(b) Variation in compressor equivalent blade tip speed and inlet Mach number with compressor rotor inlet relative Mach number (ref. 1, fig. 3(c)).

Figure 3. - Concluded. Compressor plots for maximized compressor parameter e_C.

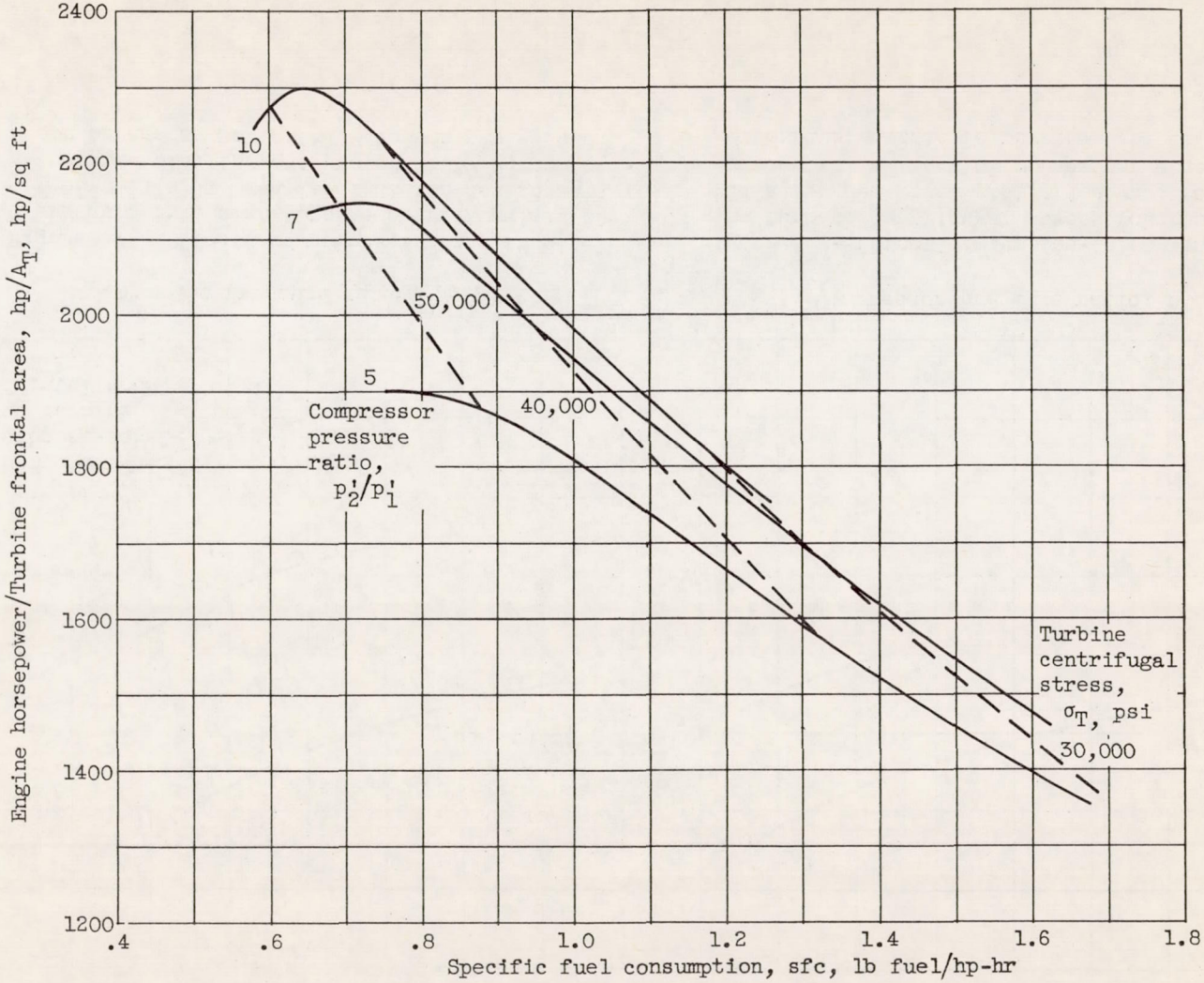

Figure 4. - Turboprop-engine performance (chart I(b)) with curves of constant stress for compressor parameter e_C of 44×10^6 pounds per second^3 for sea-level static designs at turbine-inlet temperature of 2075° R.

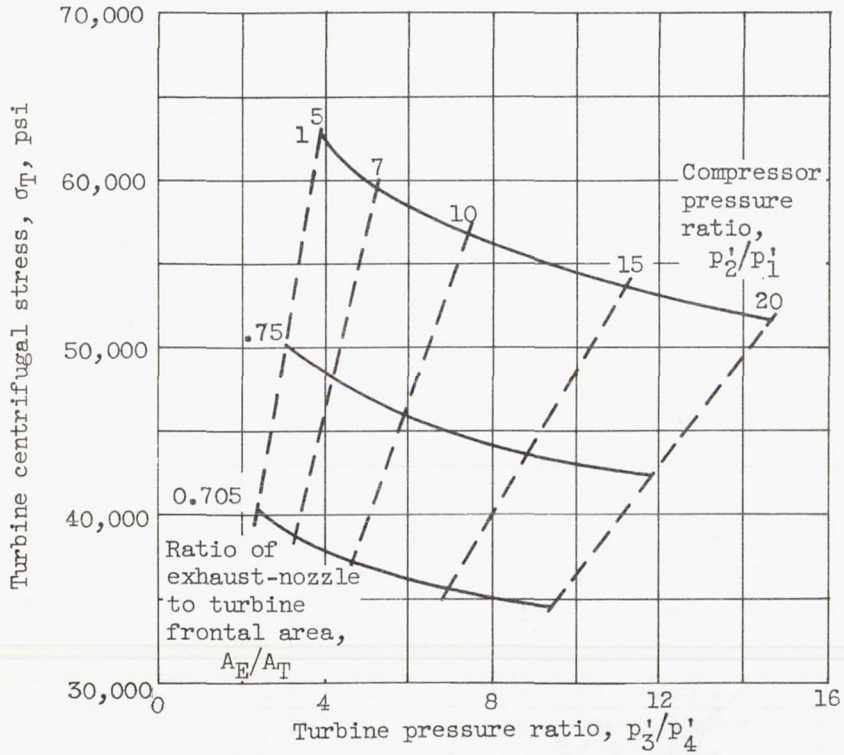

Figure 5. - Effects of compressor and turbine pressure ratios on turbine centrifugal stress (chart II(a)). Sea-level static designs at turbine-inlet temperature of 2593° R; compressor parameter e_C, 44×10^6 pounds per second^3.

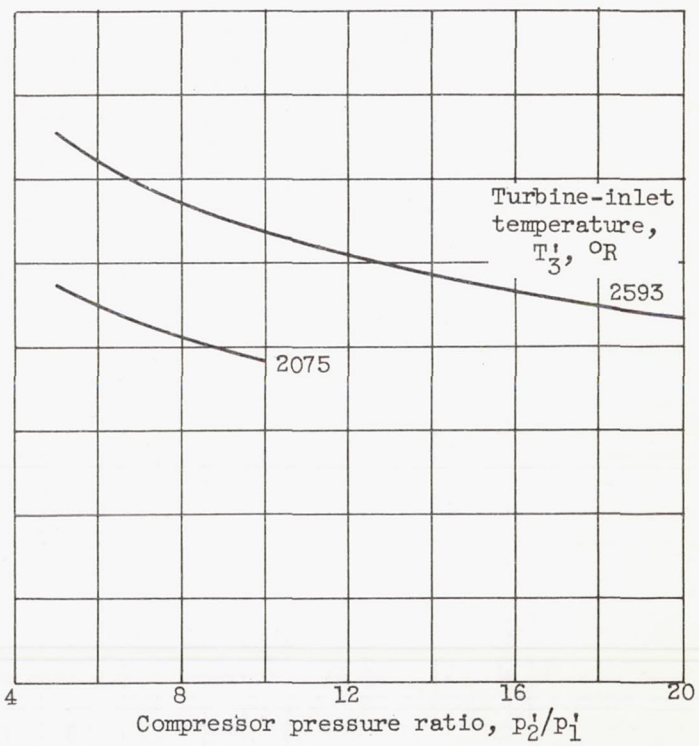

Figure 6. - Effect of turbine-inlet temperature on turbine centrifugal stress (charts I(a) and II(a)). Sea-level static designs; compressor parameter e_C, 44×10^6 pounds per second^3; ratio of exhaust-nozzle to turbine frontal area, 1.0.

4078

CU-5 back

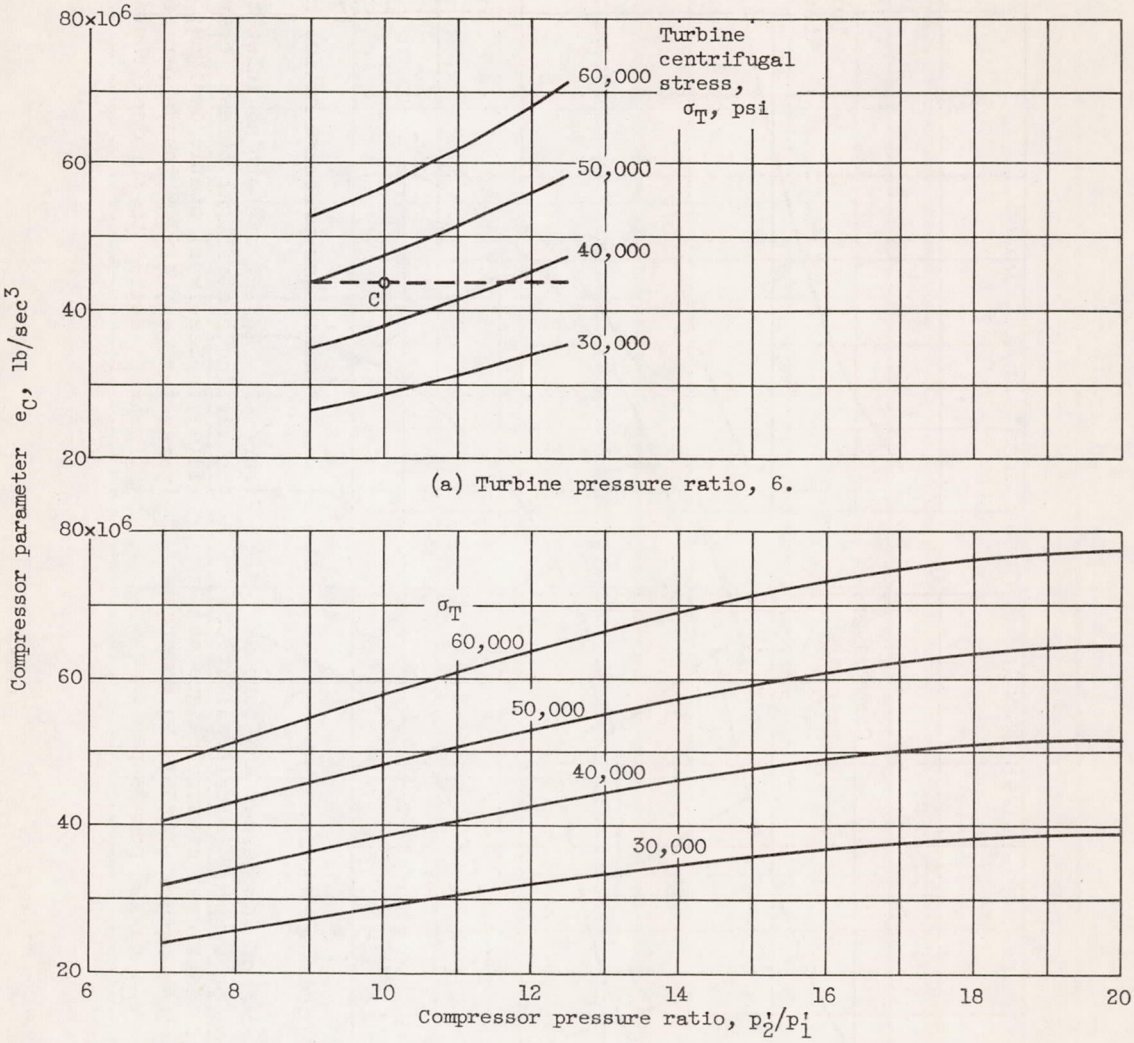

(b) Specific fuel consumption, 0.64 pound of fuel per horsepower-hour.

Figure 7. - Variation in compressor parameter e_C with compressor pressure ratio and turbine centrifugal stress (chart II). Sea-level static designs at turbine-inlet temperature of 2593° R.

4078

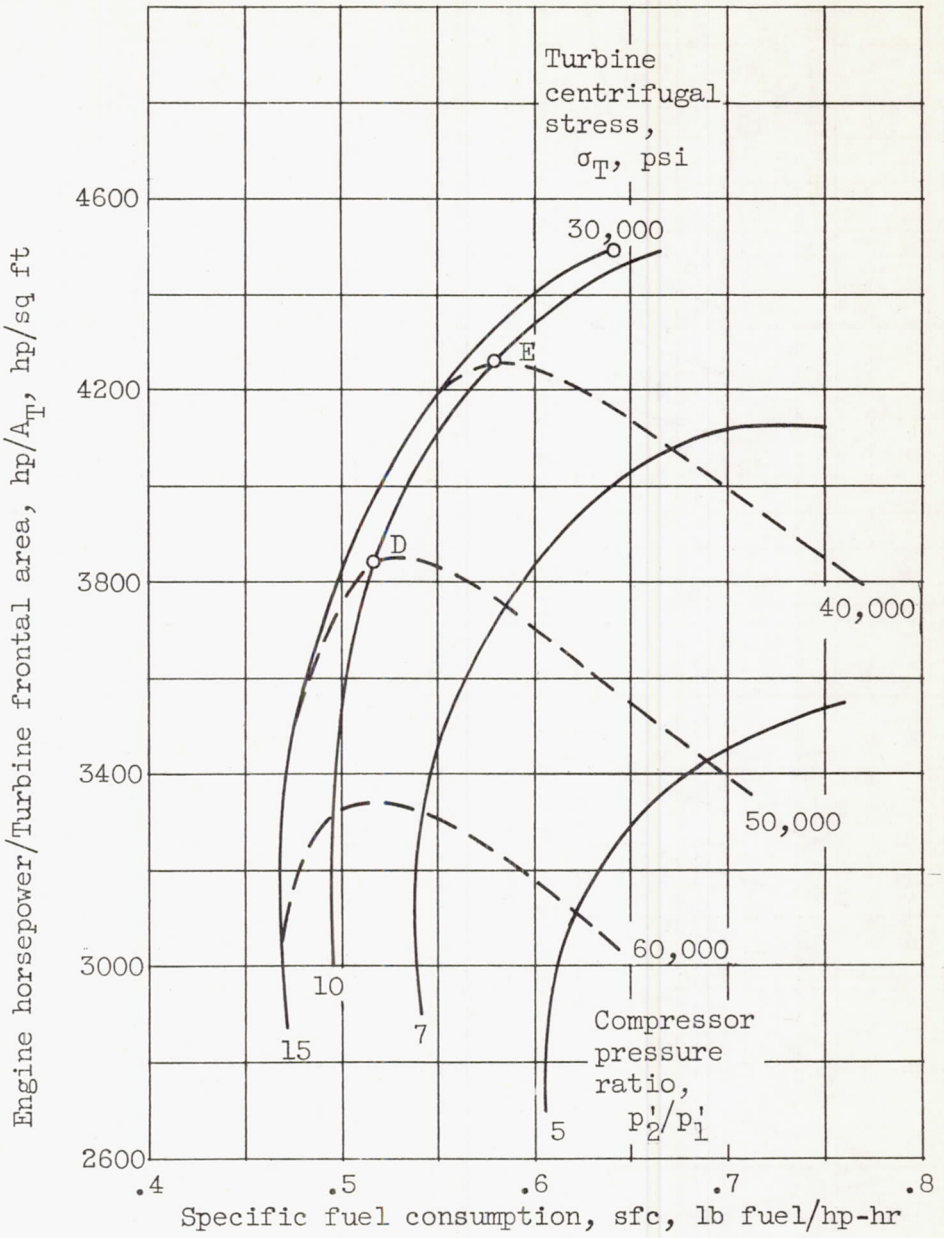

Figure 8. - Turboprop-engine performance (chart IV(b)) with curves of constant stress for compressor parameter e_C of 44×10^6 pounds per second^3 for sea-level designs at Mach 0.6 and turbine-inlet temperature of 2225° R.

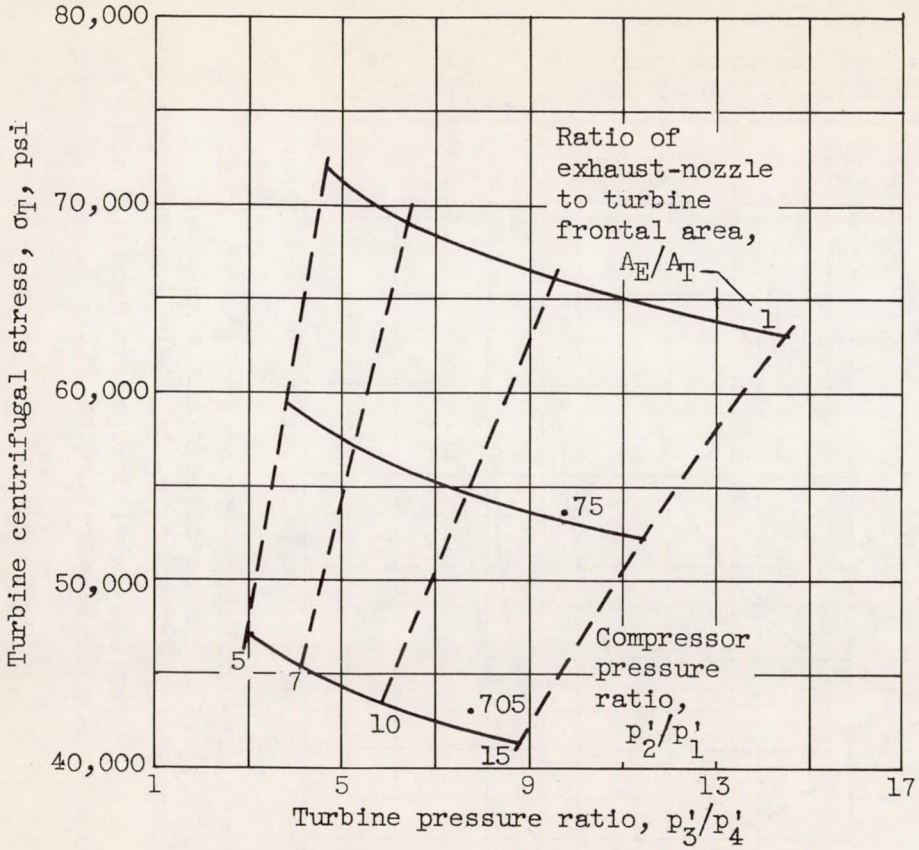

Figure 9. - Effect of compressor and turbine pressure ratios on turbine centrifugal stress for sea-level designs at Mach 0.6. turbine-inlet temperature of 2225° R, and compressor parameter e_C of 44×10^6 pounds per second^3 (chart IV(a)).

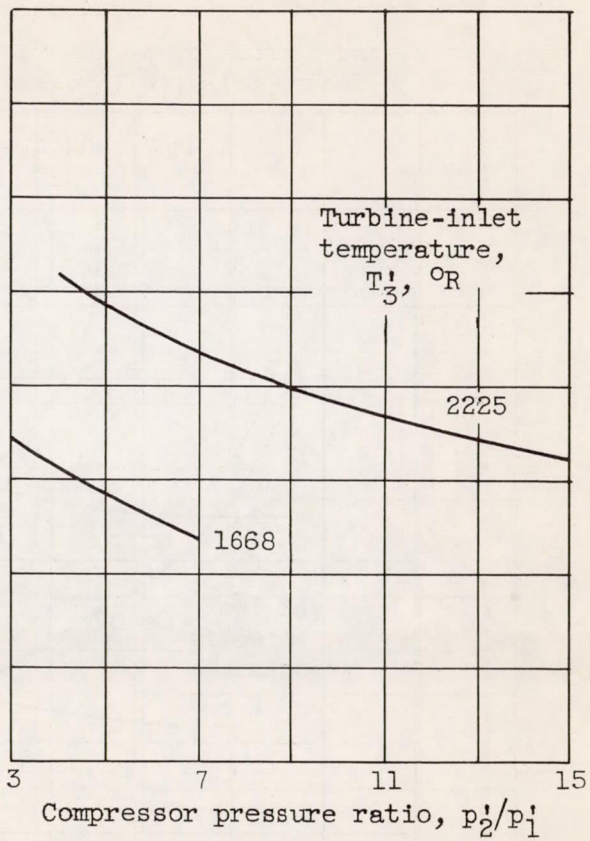

Figure 10. - Effect of turbine-inlet temperature on turbine centrifugal stress for sea-level designs at Mach 0.6, compressor parameter e_C of 44×10^6 pounds per second^3, and ratio of exhaust-nozzle to turbine frontal area of 0.8 (charts III(a) and IV(a)).

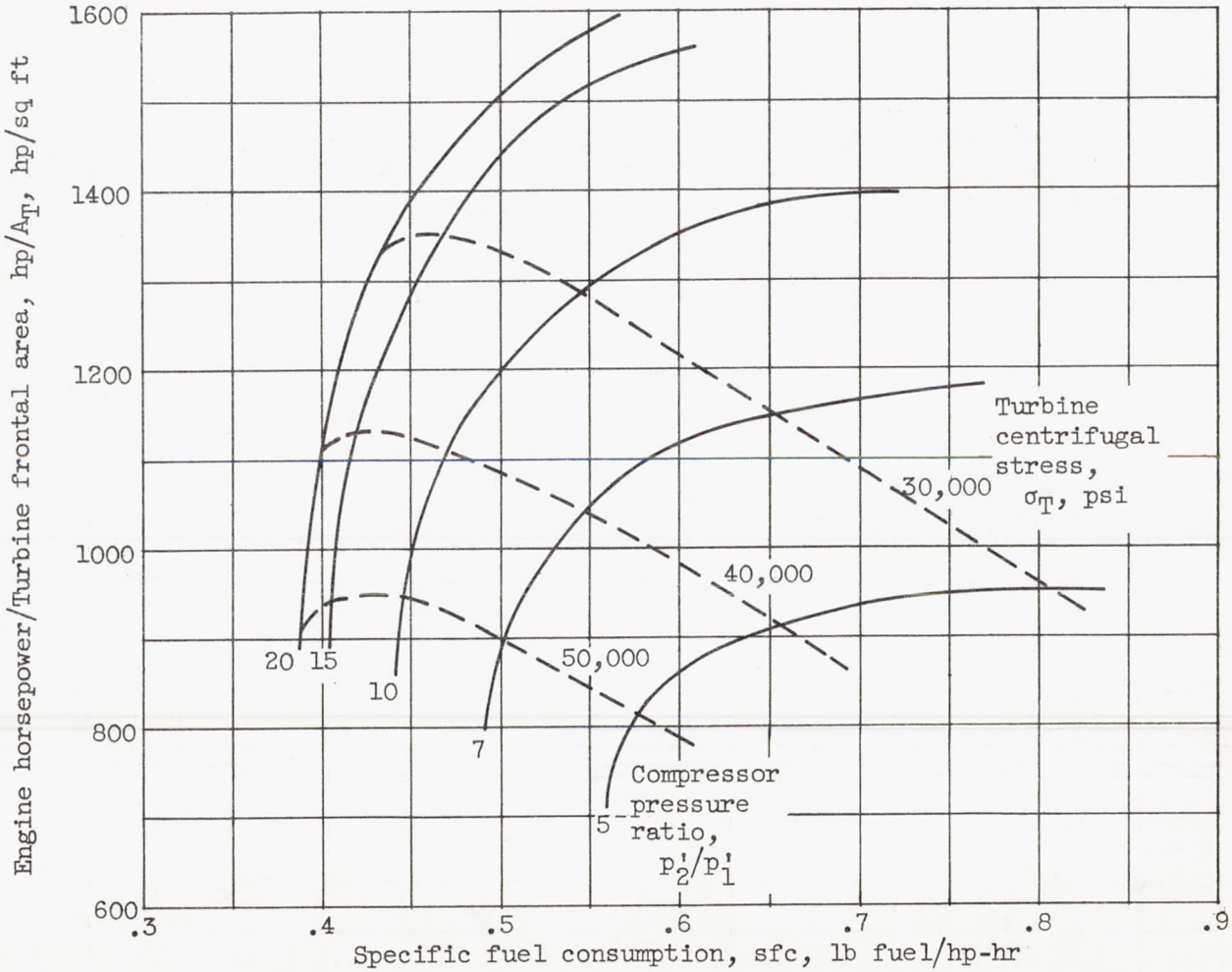

Figure 11. - Turboprop-engine performance (chart VI(b)) with curves of constant stress for compressor parameter e_C of 44×10^6 pounds per second^3 for tropopause designs at Mach number of 0.6 and turbine-inlet temperature of 2090° R.

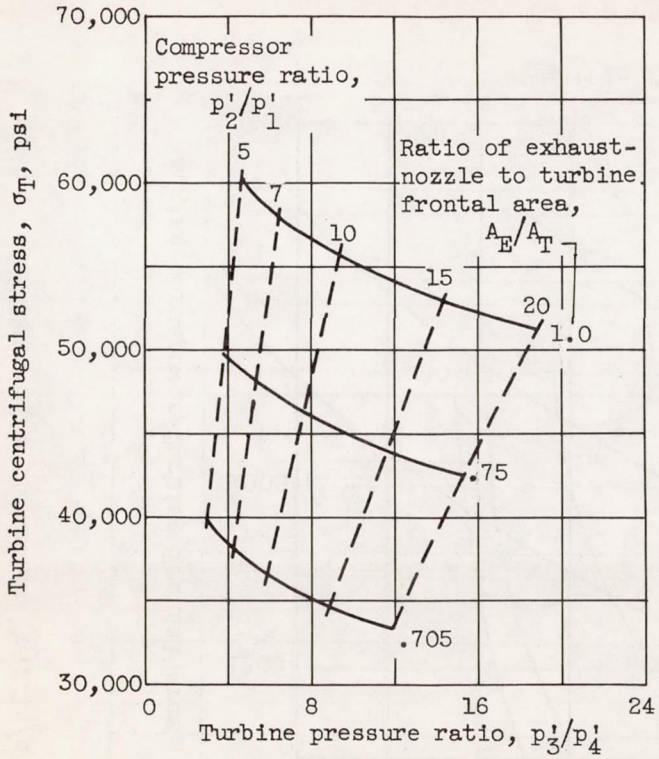

Figure 12. - Effect of compressor and turbine pressure ratios on turbine centrifugal stress for tropopause designs at Mach 0.6, turbine-inlet temperature of 2090° R, and compressor parameter e_C of 44×10^6 pounds per second^3 (chart VI(a)).

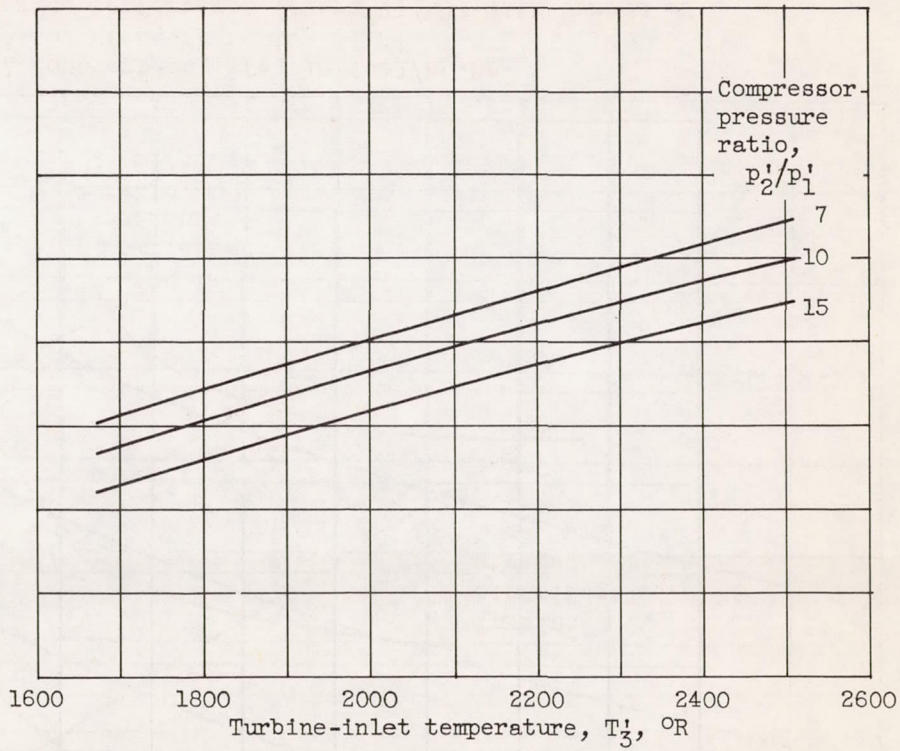

Figure 13. - Effect of turbine-inlet temperature on turbine centrifugal stress for tropopause designs at Mach 0.6, compressor parameter of 44×10^6 pounds per second^3, and ratio of exhaust-nozzle to turbine frontal area of 0.8 (charts V(a), VI(a), and VII(a)).

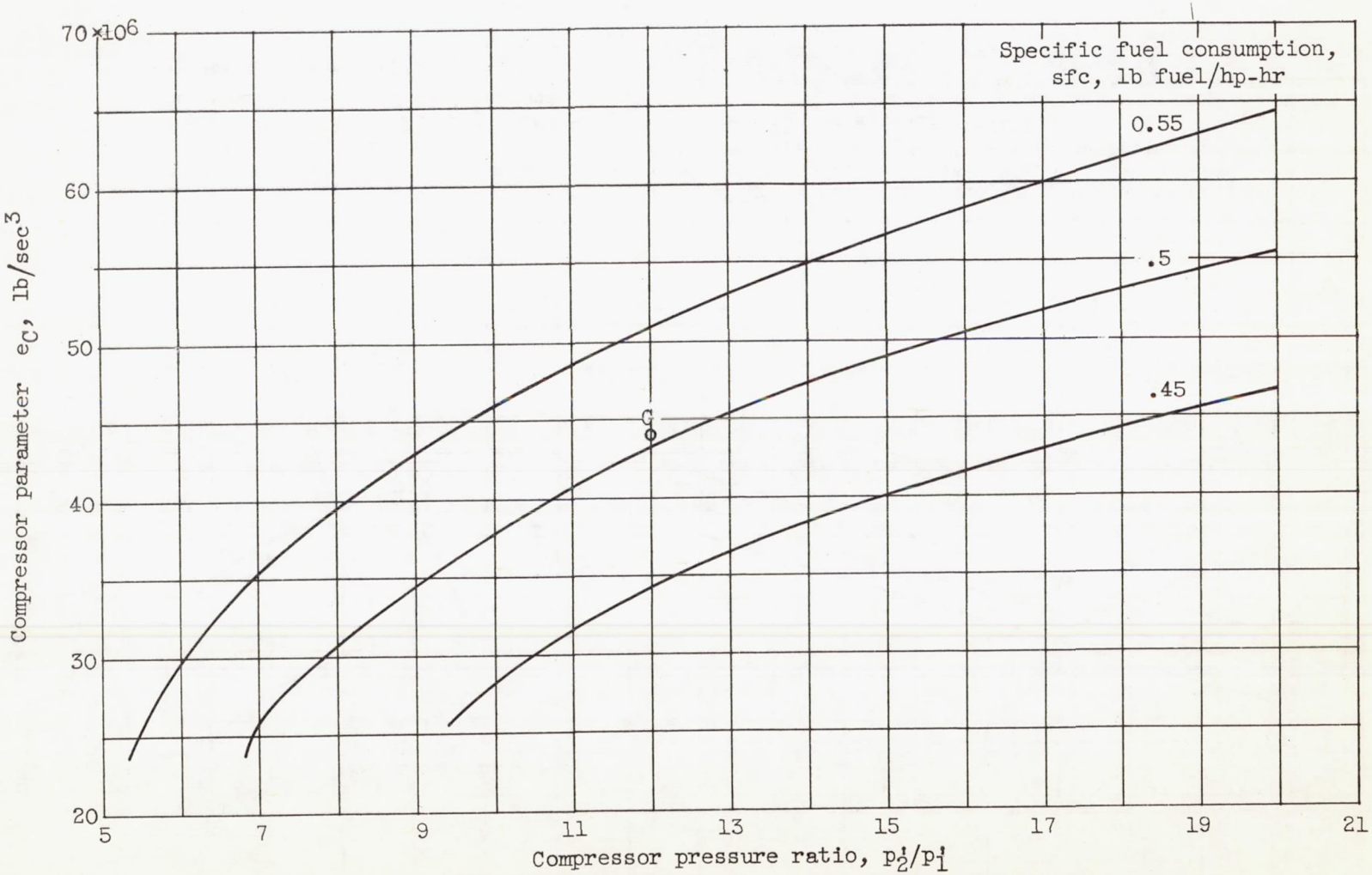

Figure 14. - Variation in compressor parameter e_C with compressor pressure ratio and specific fuel consumption for constant turbine stress of 30,000 pounds per square inch (chart VI). Tropopause designs; Mach number, 0.6; turbine-inlet temperature, 2090° R.

4078

CU-6

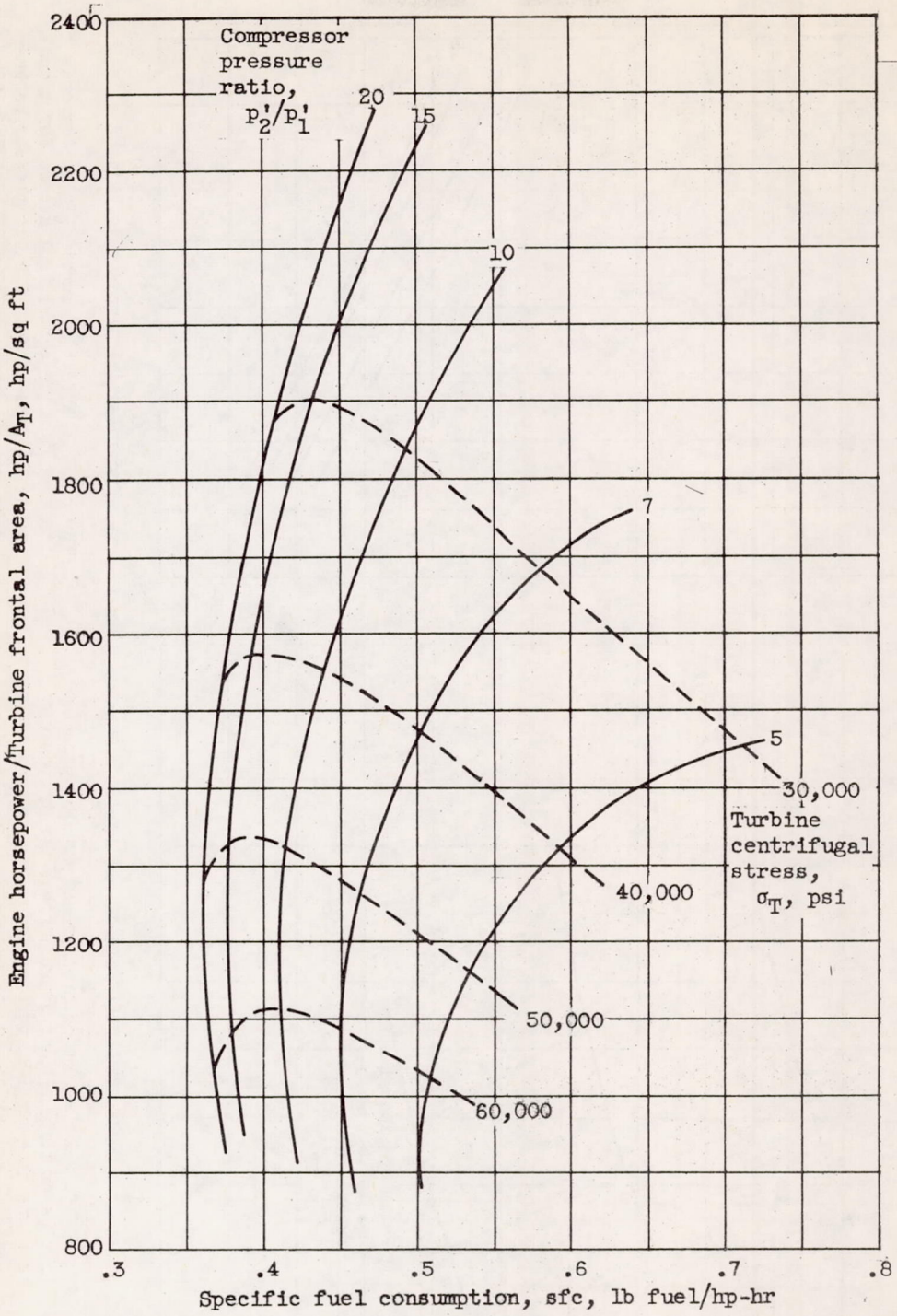

Figure 15. - Turboprop-engine performance (chart IX(b)) with curves of constant stress for compressor parameter e_C of 44×10^6 pounds per second^3. Tropopause designs; Mach number, 0.8; turbine-inlet temperature, 2200° R.

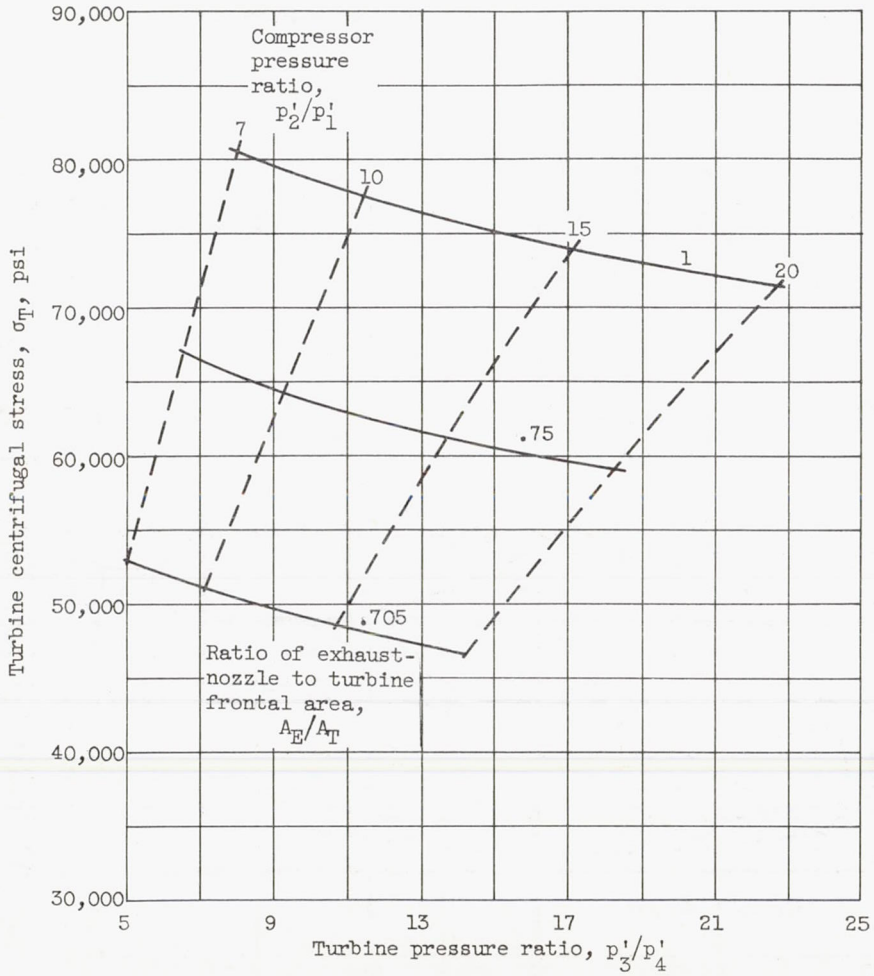

Figure 16. - Effect of compressor and turbine pressure ratios on turbine centrifugal stress for tropopause designs at Mach 0.8, turbine-inlet temperature of 2641° R, and compressor parameter e_C of 44×10^6 pounds per second^3 (chart X(a)).

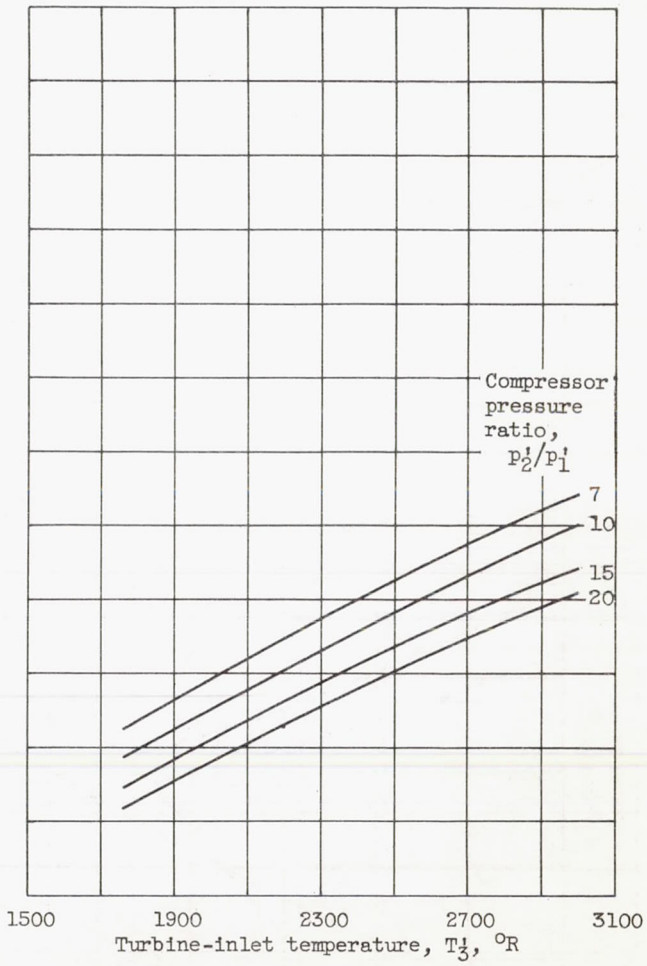

Figure 17. - Effect of turbine-inlet temperature on turbine centrifugal stress for tropopause designs at Mach 0.8, compressor parameter e_C of 44×10^6 pounds per second^3, and ratio of exhaust-nozzle to turbine frontal area of 0.705 (exhaust nozzle just choking) (charts VIII(a), IX(a), X(a), and XI(a)).

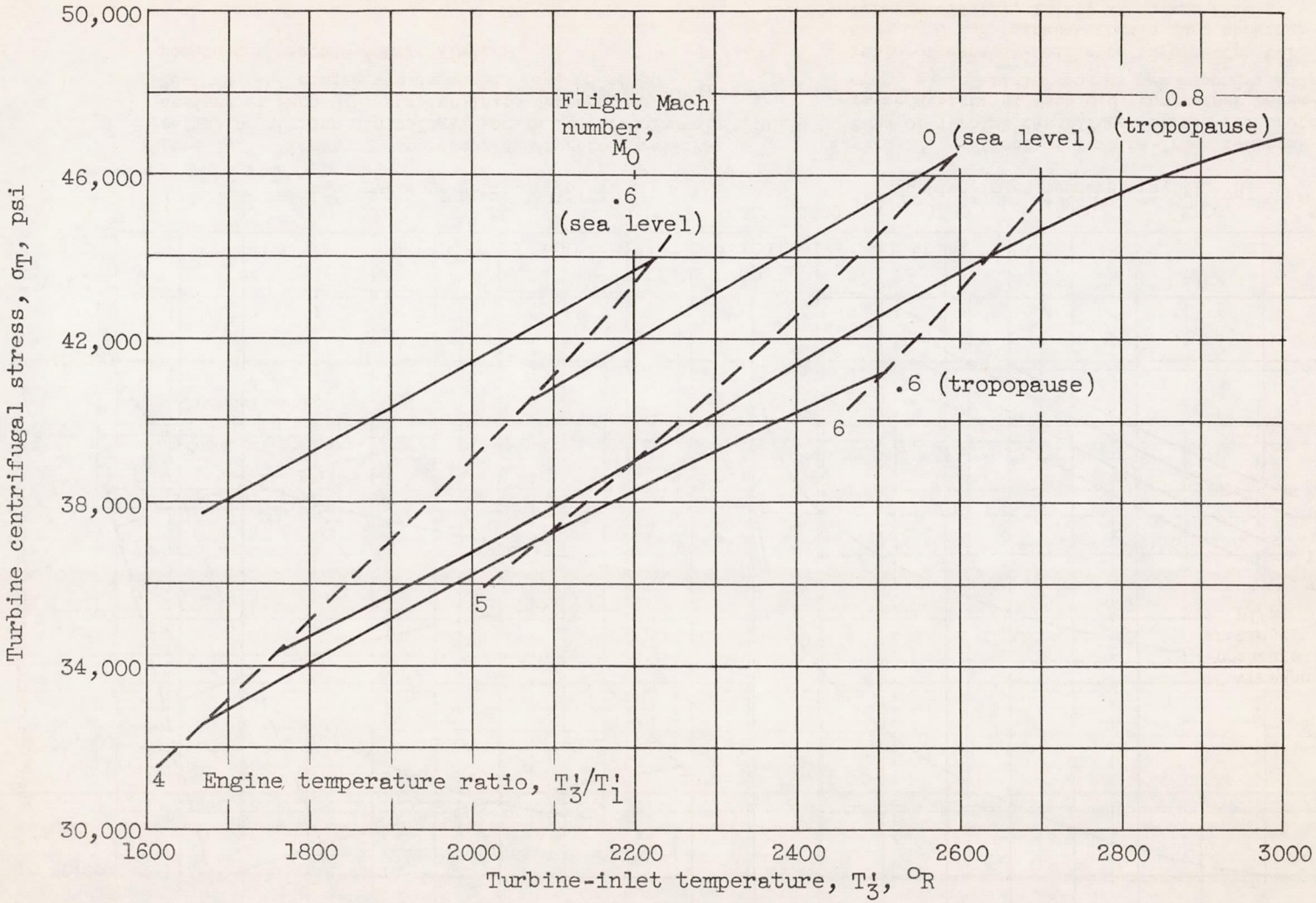

Figure 18. - Effect of flight conditions on turbine centrifugal stress. Compressor parameter e_C, 44×10^6 pounds per second^3; compressor pressure ratio, 10; turbine pressure ratio, 6.

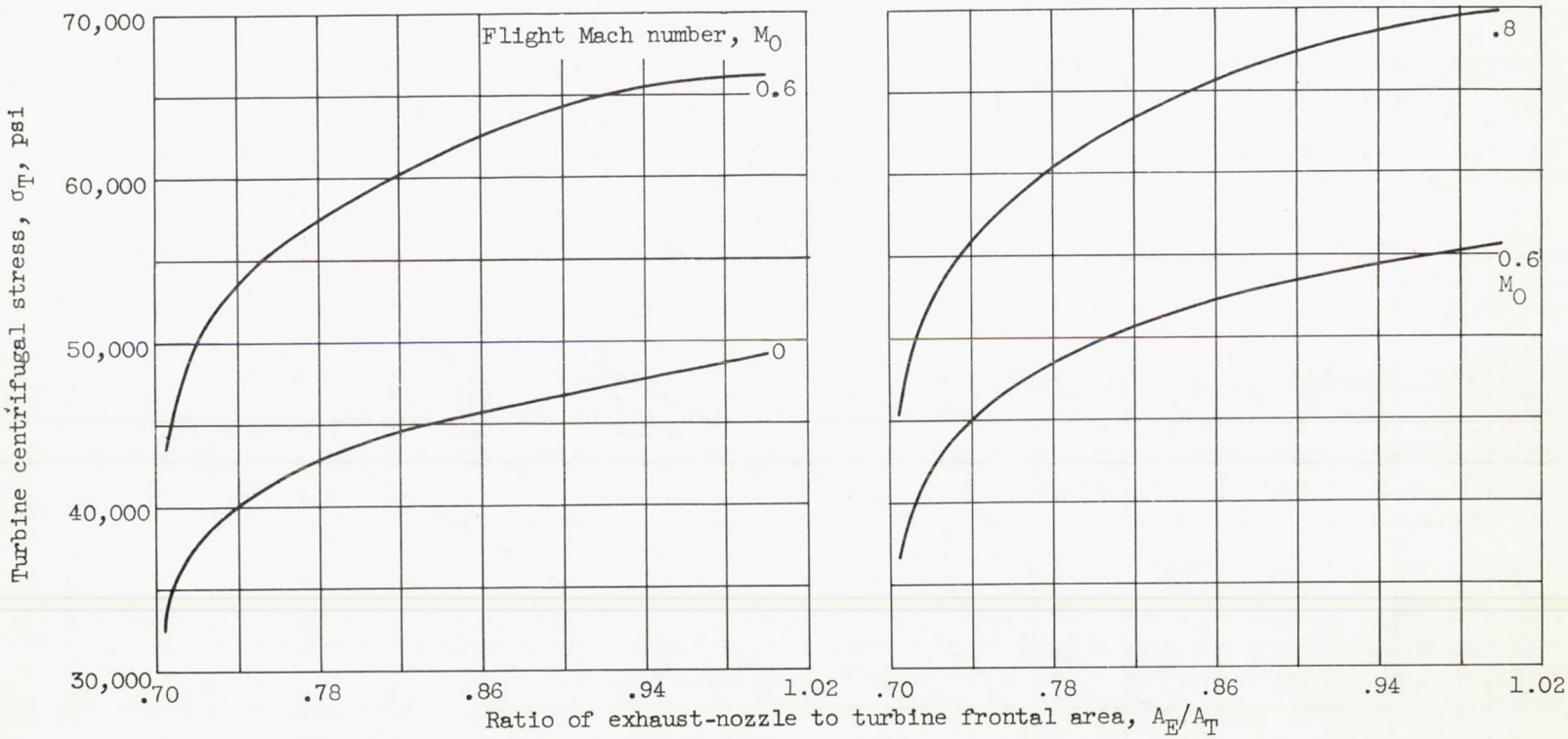

(a) Sea-level designs; engine temperature ratio, 4.

(b) Tropopause designs; engine temperature ratio, 5.

Figure 19. - Effect of A_E/A_T and flight Mach number on turbine centrifugal stress. Compressor parameter e_C, 44×10^6 pounds per second^3; compressor pressure ratio, 10.

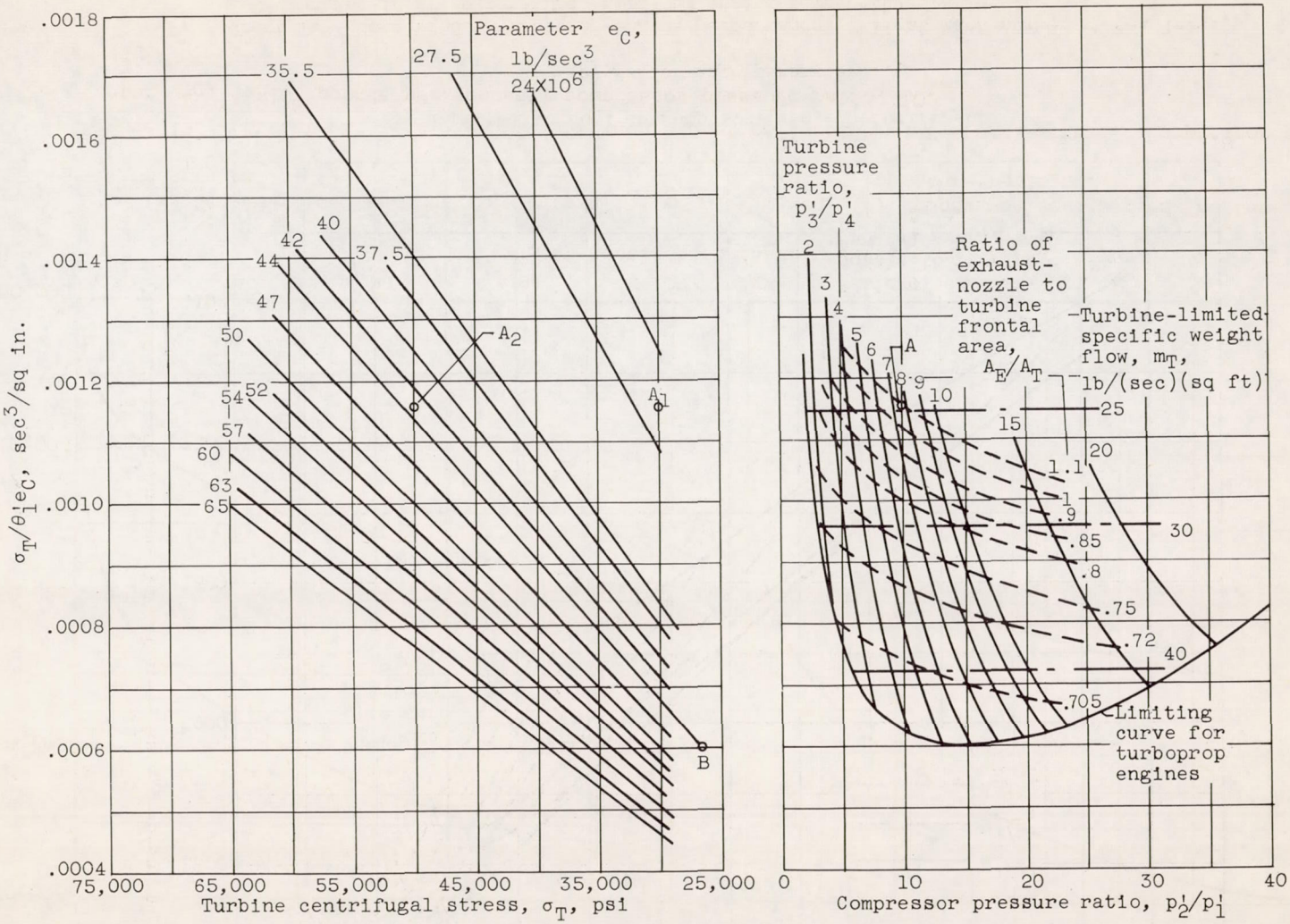

(a) Engine parameters.

Chart I. - Turboprop-engine performance. Flight Mach number at sea level, 0; turbine-inlet temperature, 2075° R; engine temperature ratio, 4.

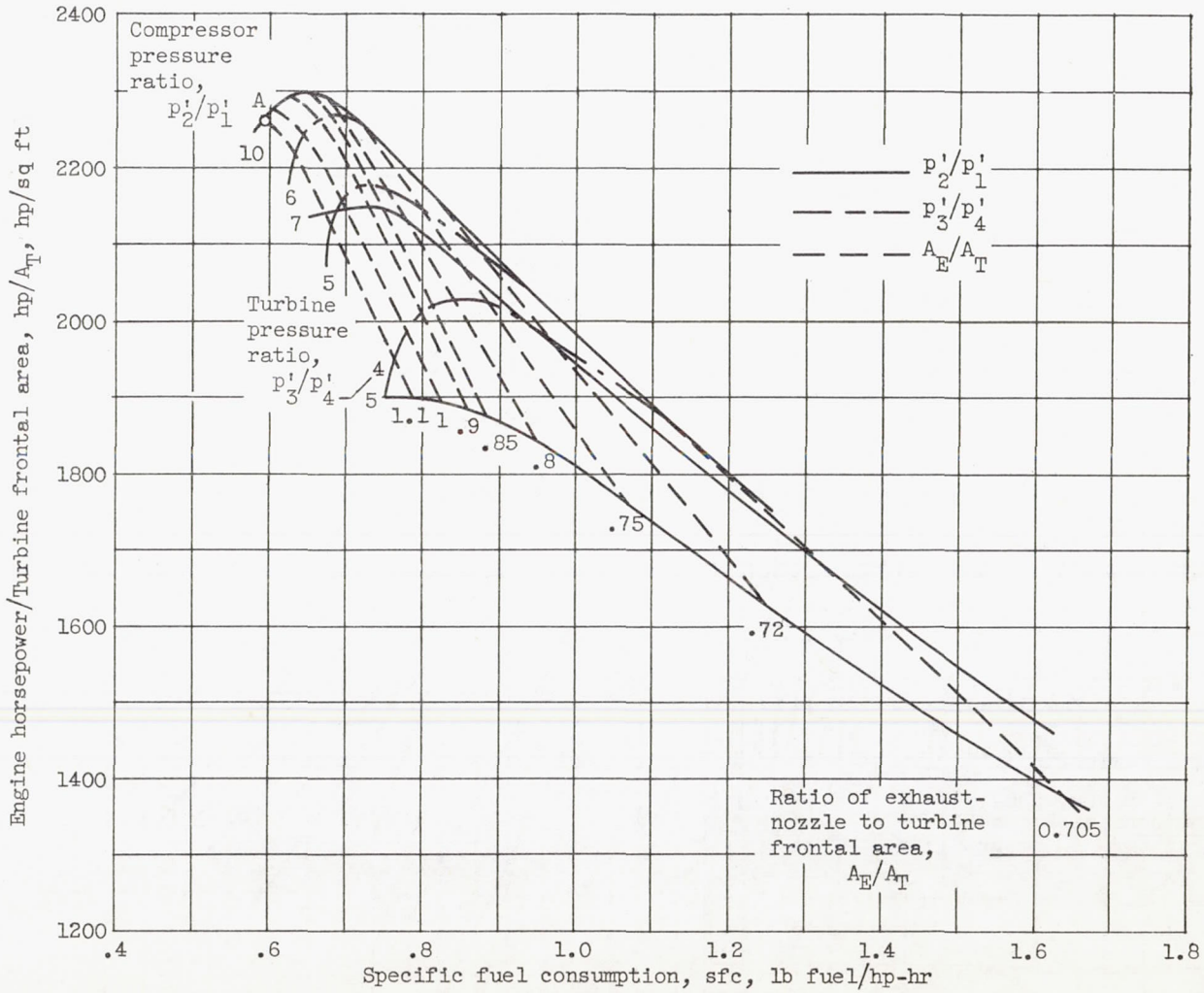

(b) Performance parameters.

Chart I. - Concluded. Turboprop-engine performance. Flight Mach number at sea level, 0; turbine-inlet temperature, 2075° R; engine temperature ratio, 4.

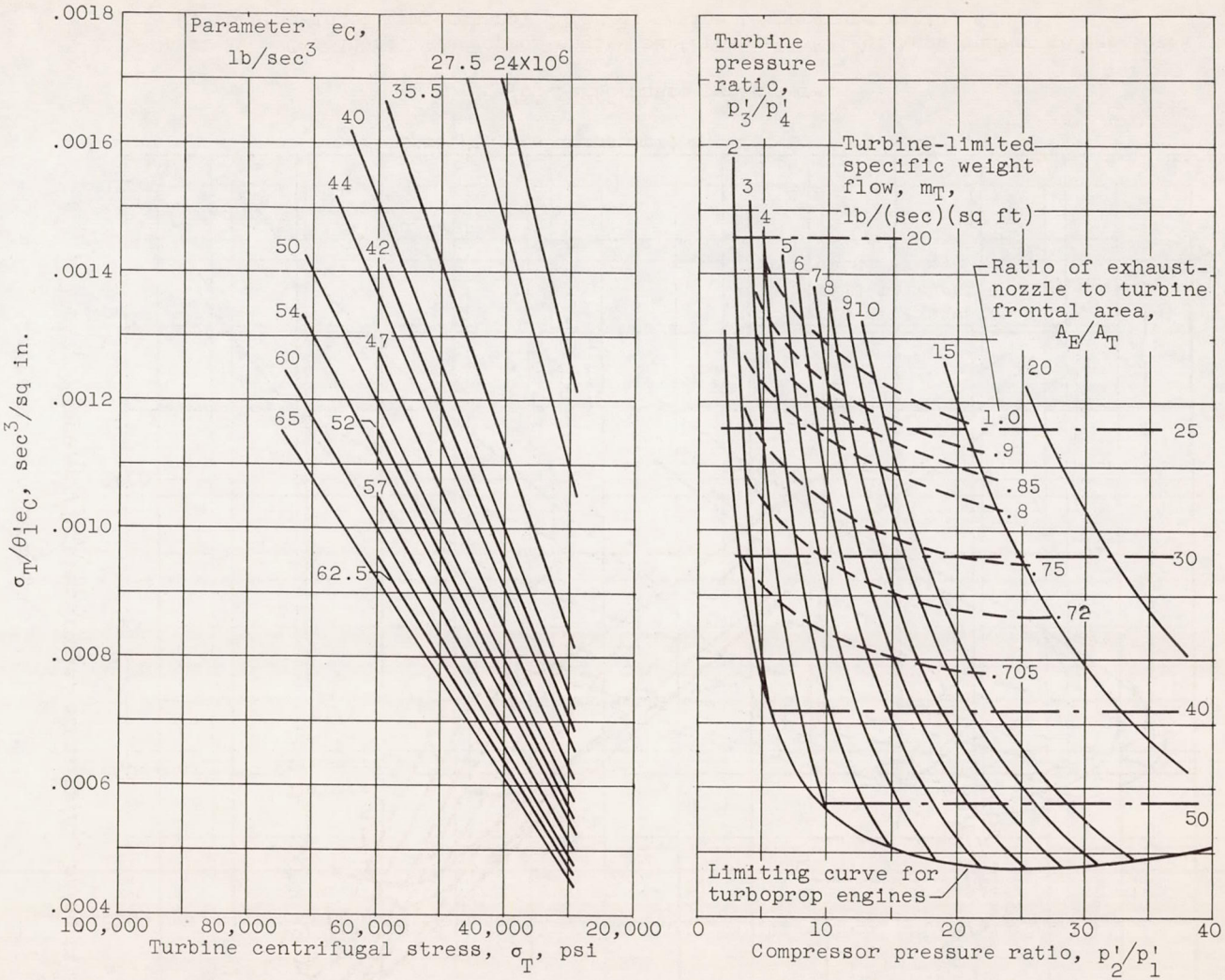

(a) Engine parameters.

Chart II. - Turboprop-engine performance. Flight Mach number at sea level, 0; turbine-inlet temperature, 2593° R; engine temperature ratio, 5.

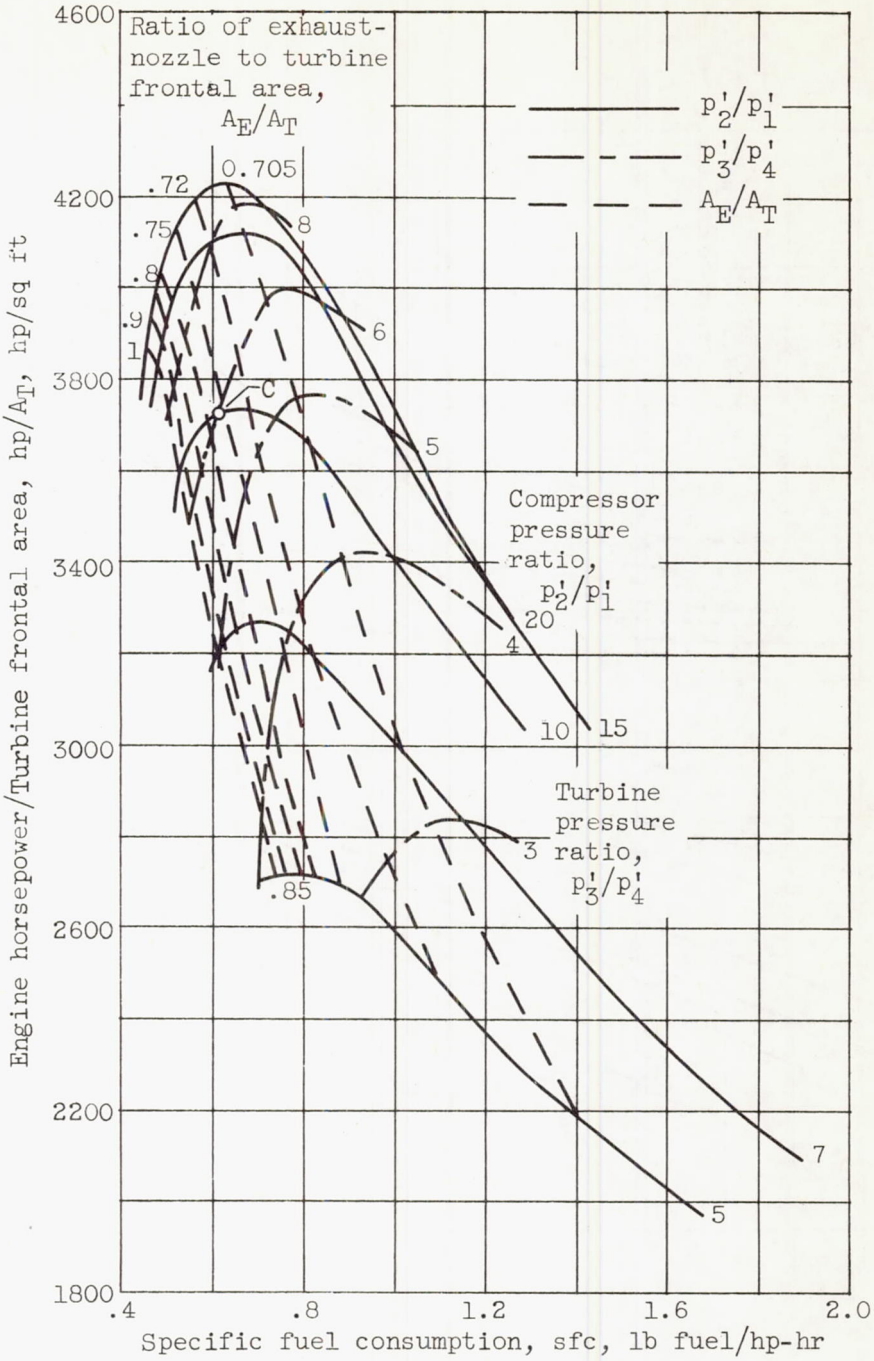

(b) Performance parameters.

Chart II. - Concluded. Turboprop-engine performance. Flight Mach number at sea level, 0; turbine-inlet temperature, 2593° R; engine temperature ratio, 5.

4078

4078

CU-7

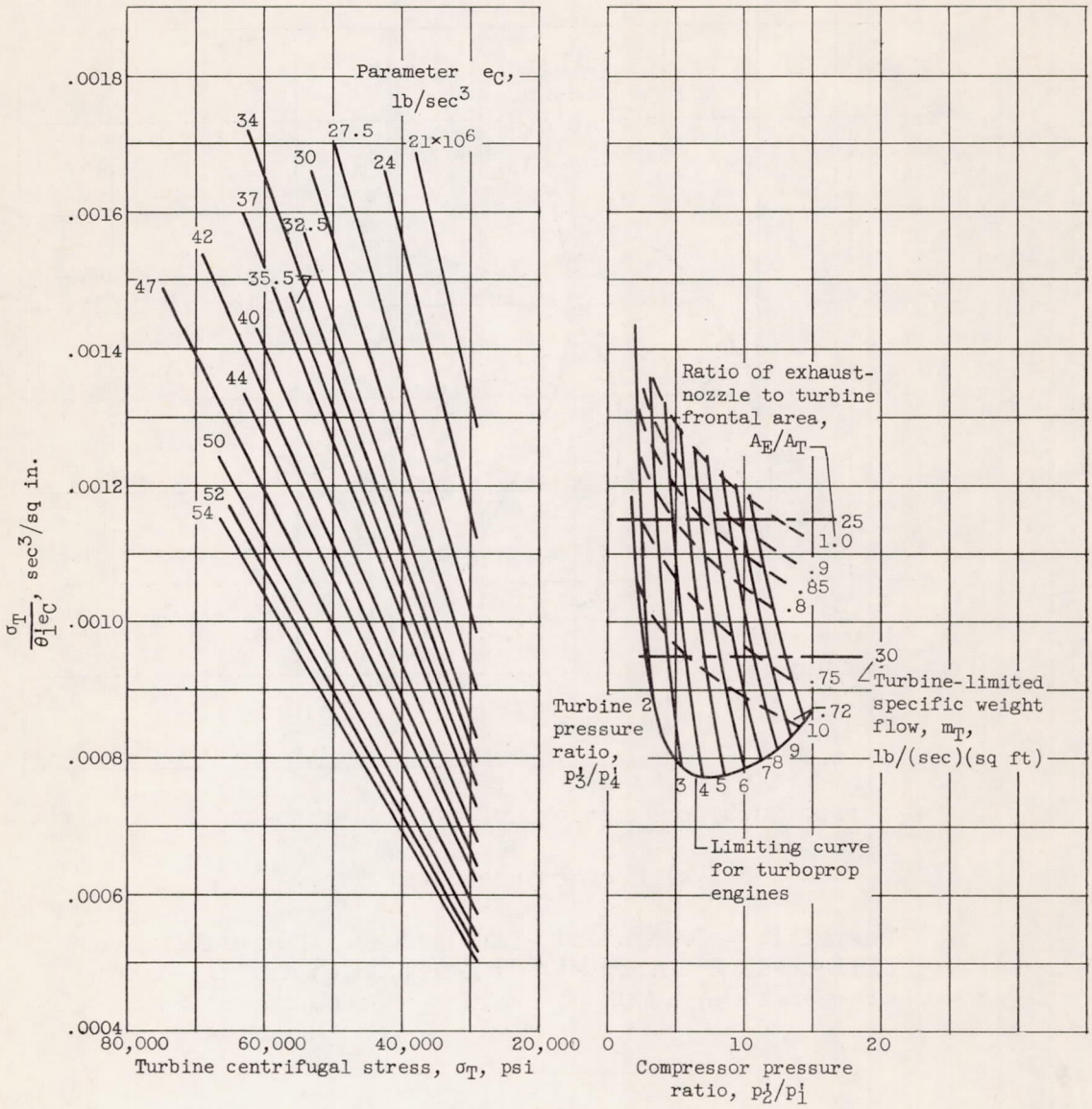

(a) Engine parameters.

Chart III. - Turboprop-engine performance. Flight Mach number at sea level, 0.6; turbine-inlet temperature, 1668° R; engine temperature ratio, 3.

4078

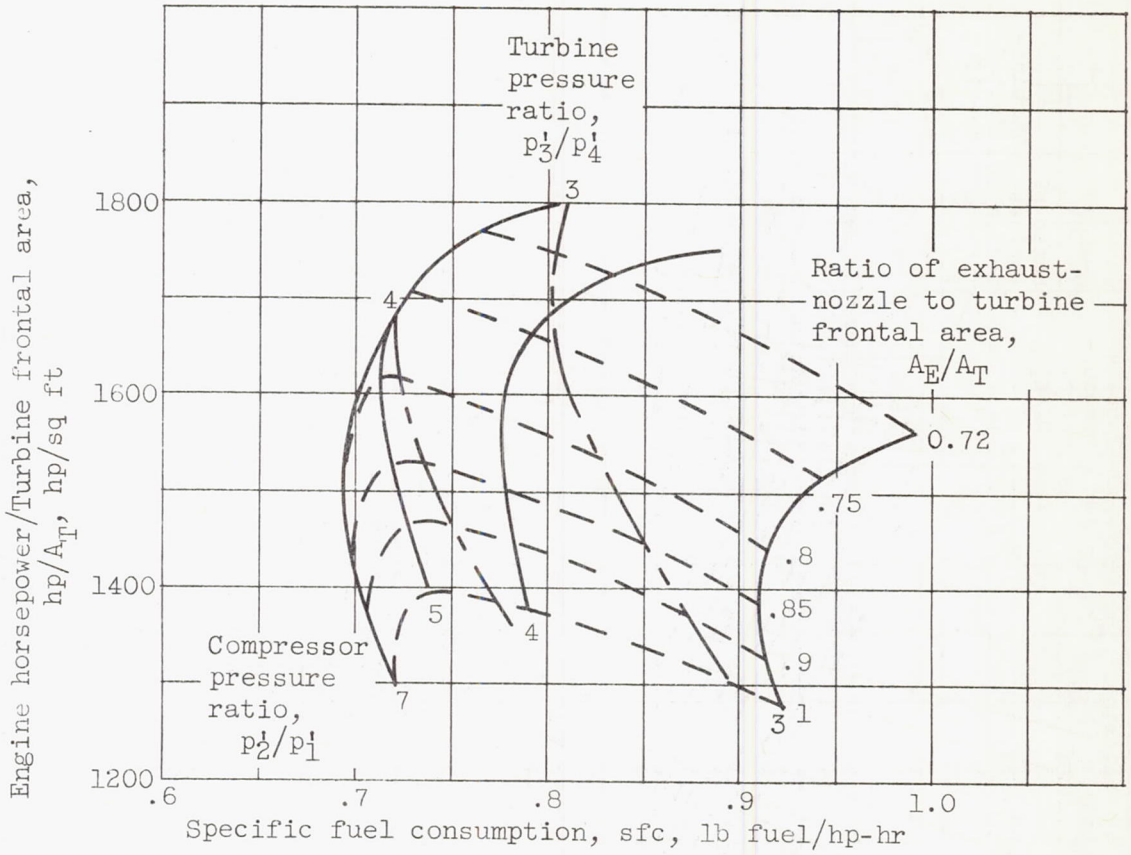

(b) Performance parameters.

Chart III. - Concluded. Turboprop-engine performance. Flight Mach number at sea level, 0.6; turbine-inlet temperature, 1668° R; engine temperature ratio, 3.

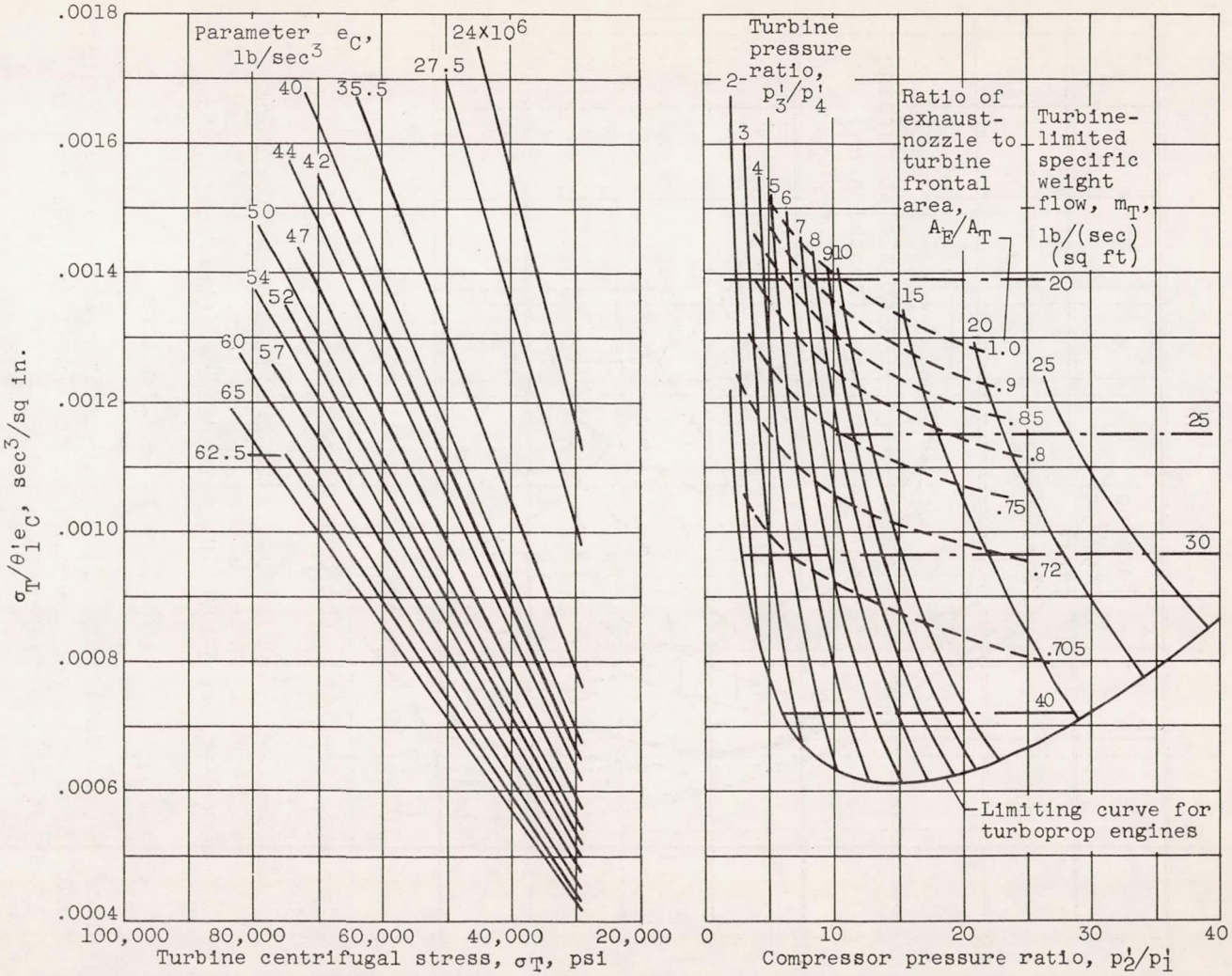

(a) Engine parameters.

Chart IV. - Turboprop-engine performance. Flight Mach number at sea level, 0.6; turbine-inlet temperature, 2225° R; engine temperature ratio, 4.

4078

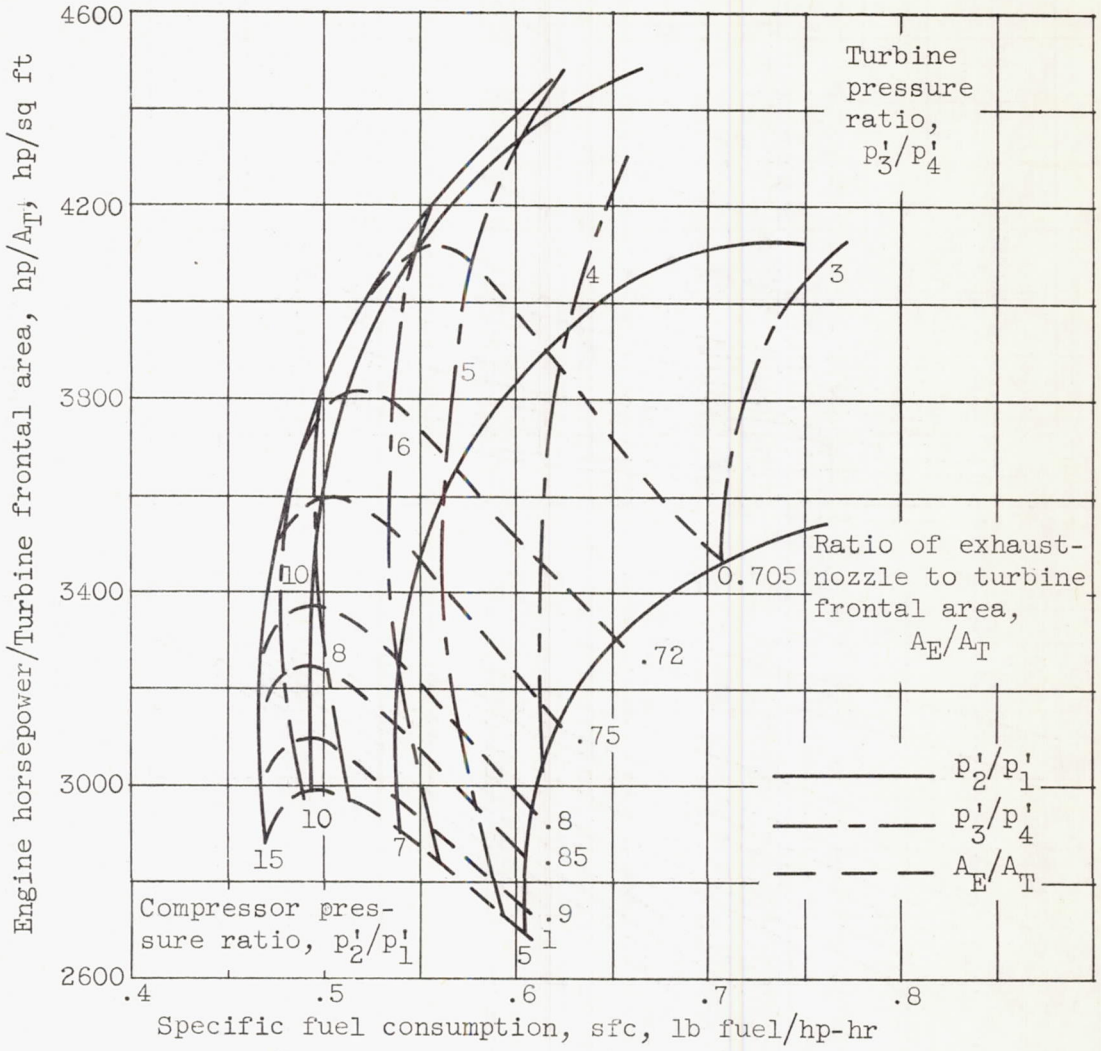

(b) Performance parameters.

Chart IV. - Concluded. Turboprop-engine performance. Flight Mach number at sea level, 0.6; turbine-inlet temperature, 2225° R; engine temperature ratio, 4.

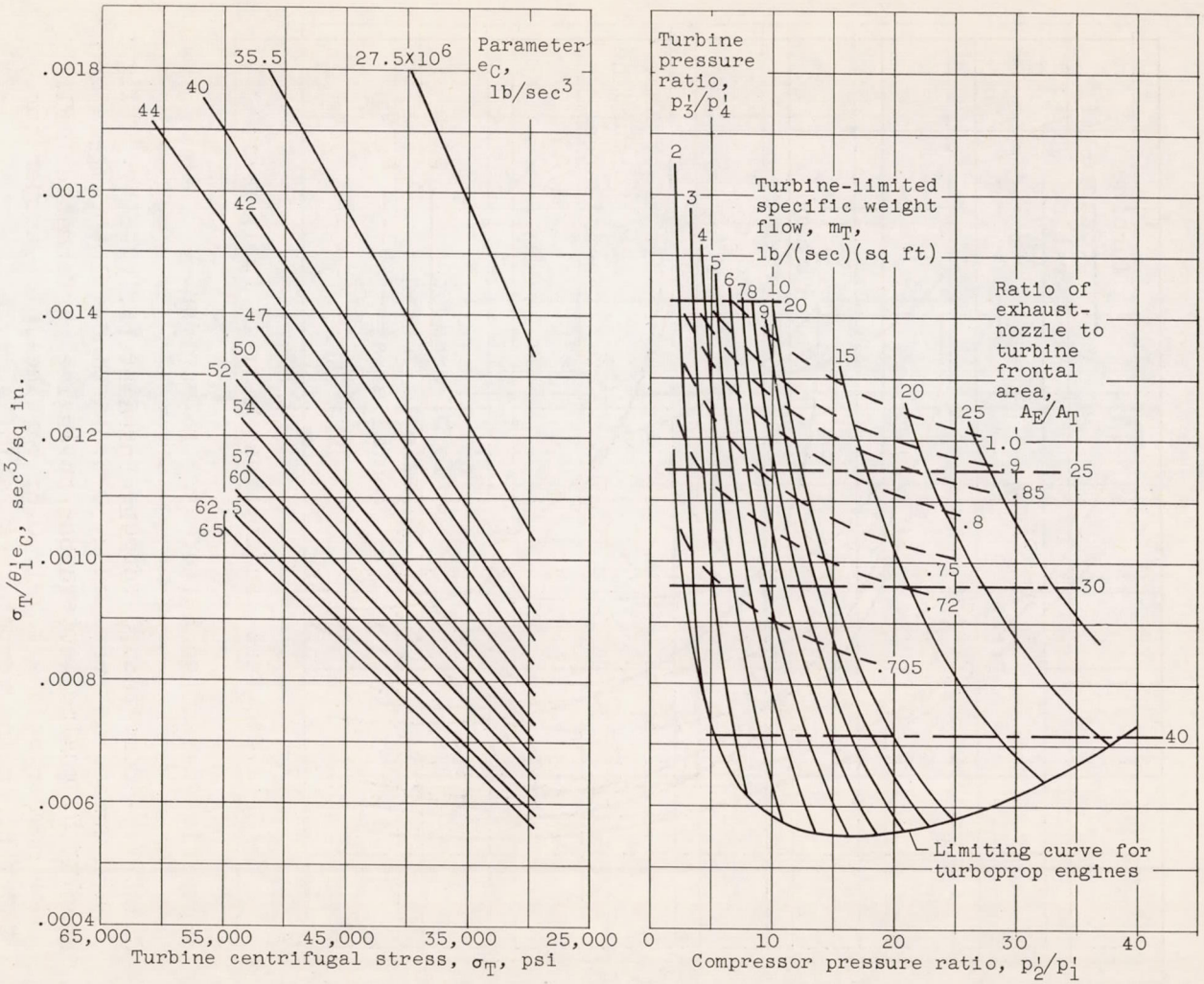

(a) Engine parameters.

Chart V. - Turboprop-engine performance. Flight Mach number at tropopause, 0.6; turbine-inlet temperature, 1672° R; engine temperature ratio, 4.

4078

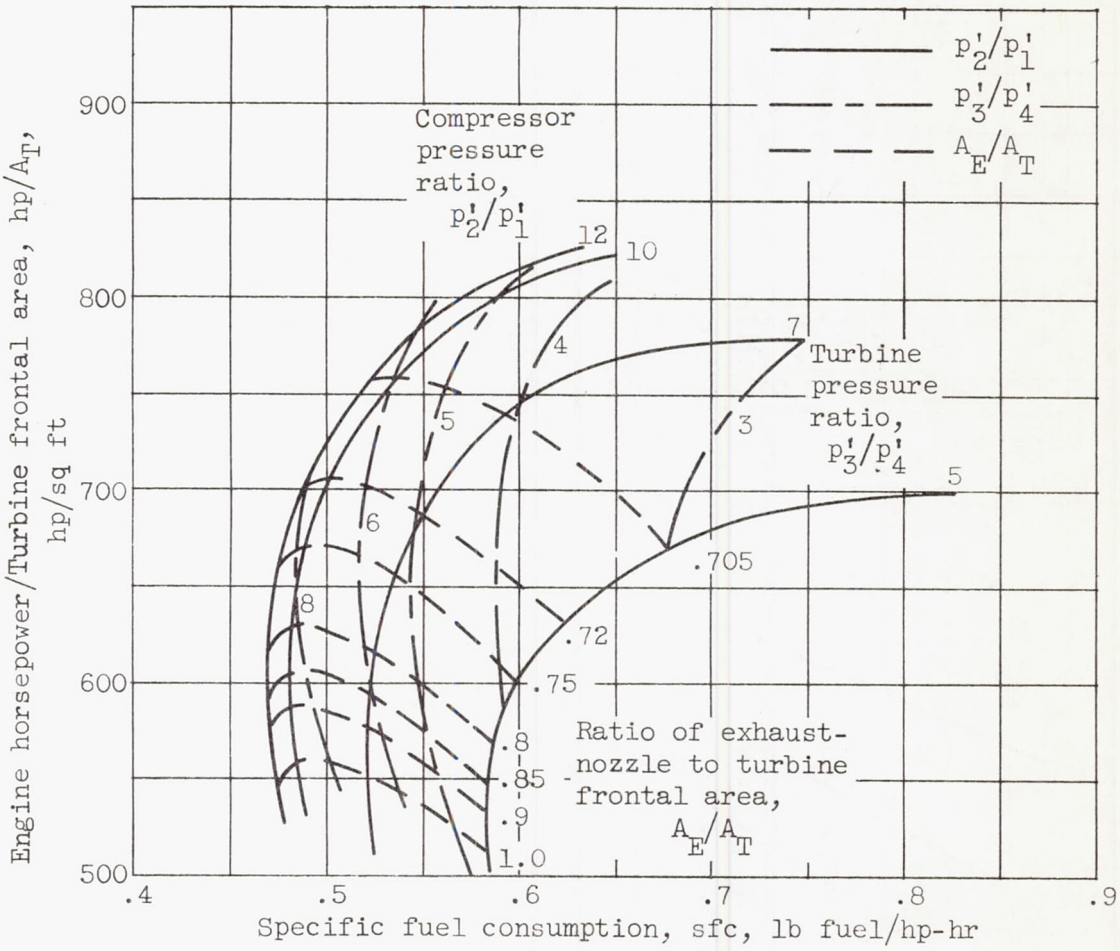

(b) Performance parameters.

Chart V. - Concluded. Turboprop-engine performance. Flight Mach number at tropopause, 0.6; turbine-inlet temperature, 1672° R; engine temperature ratio, 4.

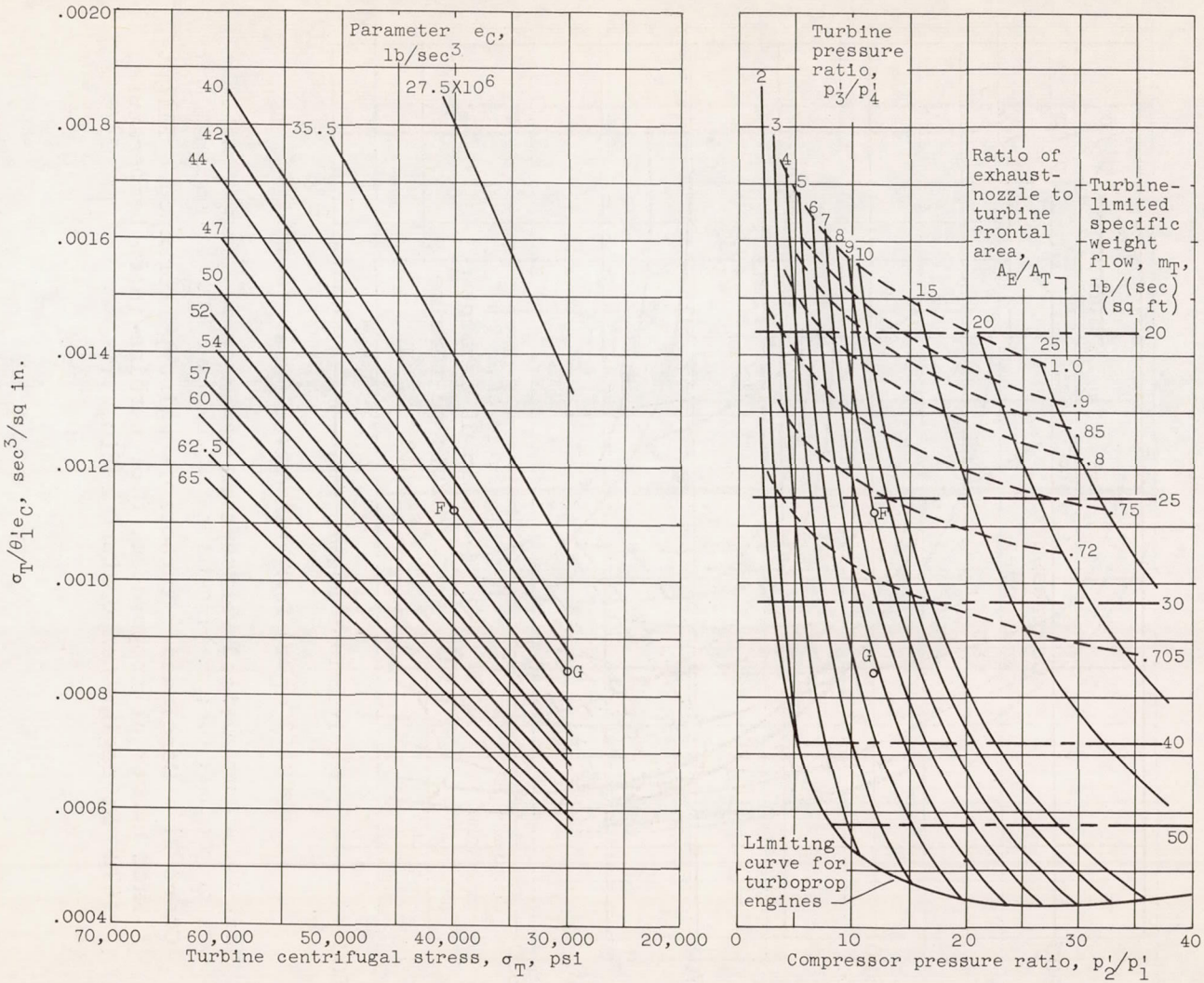

(a) Engine parameters.

Chart VI. - Turboprop-engine performance. Flight Mach number at tropopause, 0.6; turbine-inlet temperature, 2090° R; engine temperature ratio, 5.

4078

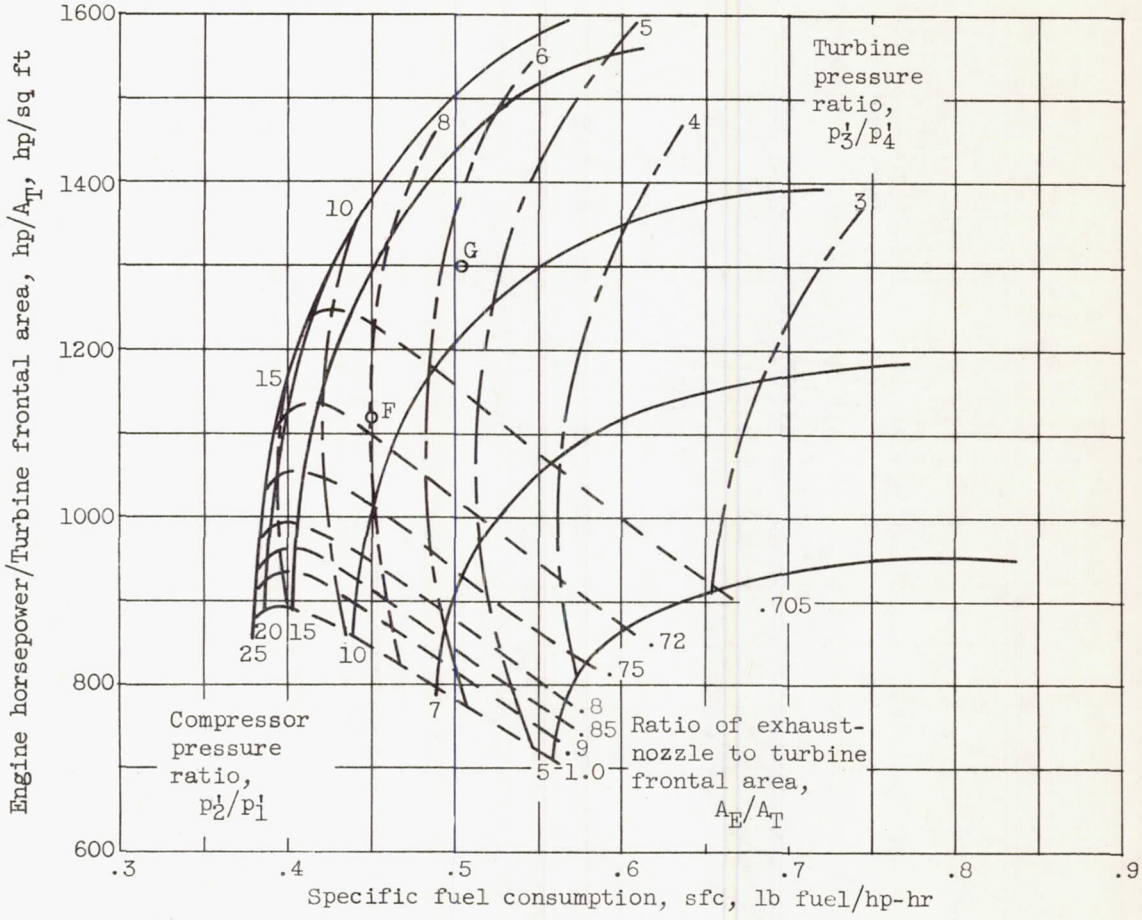

(b) Performance parameters.

Chart VI. - Concluded. Turboprop-engine performance. Flight Mach number at tropopause, 0.6; turbine-inlet temperature, 2090° R; engine temperature ratio, 5.

4078

CU-8

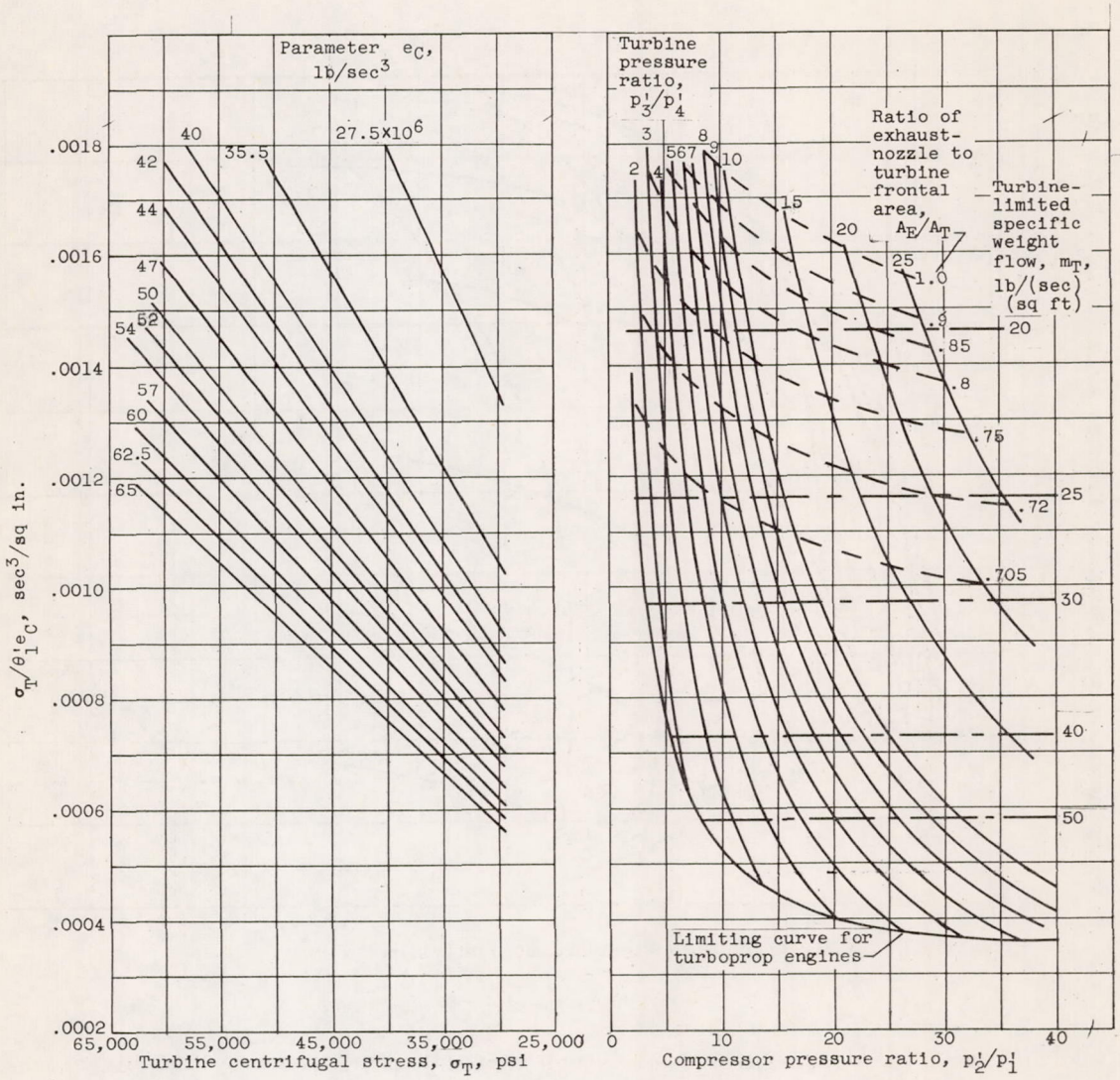

(a) Engine parameters.

Chart VII. - Turboprop-engine performance. Flight Mach number at tropopause, 0.6; turbine-inlet temperature, 2509° R; engine temperature ratio, 6.

4078

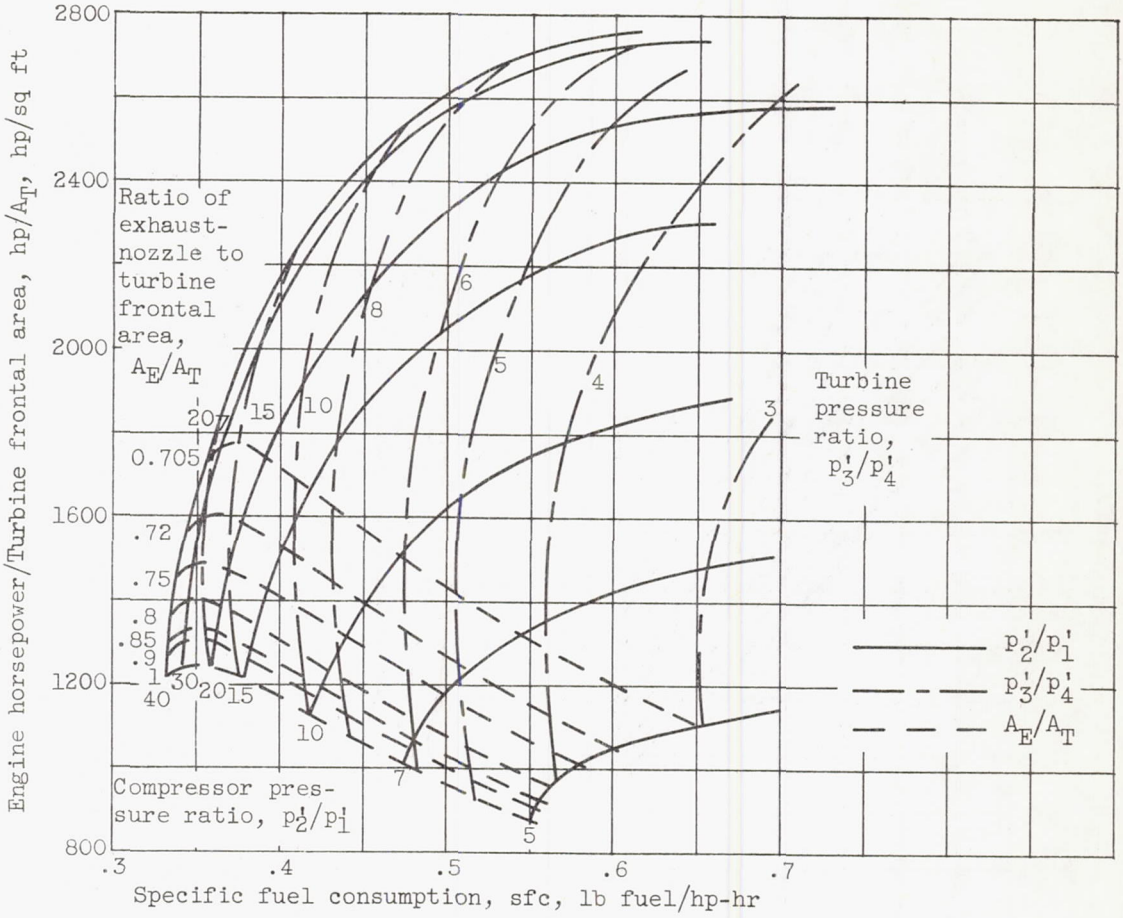

(b) Performance parameters.

Chart VII. - Concluded. Turboprop-engine performance. Flight Mach number at tropopause, 0.6; turbine-inlet temperature, 2509° R; engine temperature ratio, 6.

4078

CU-8 back

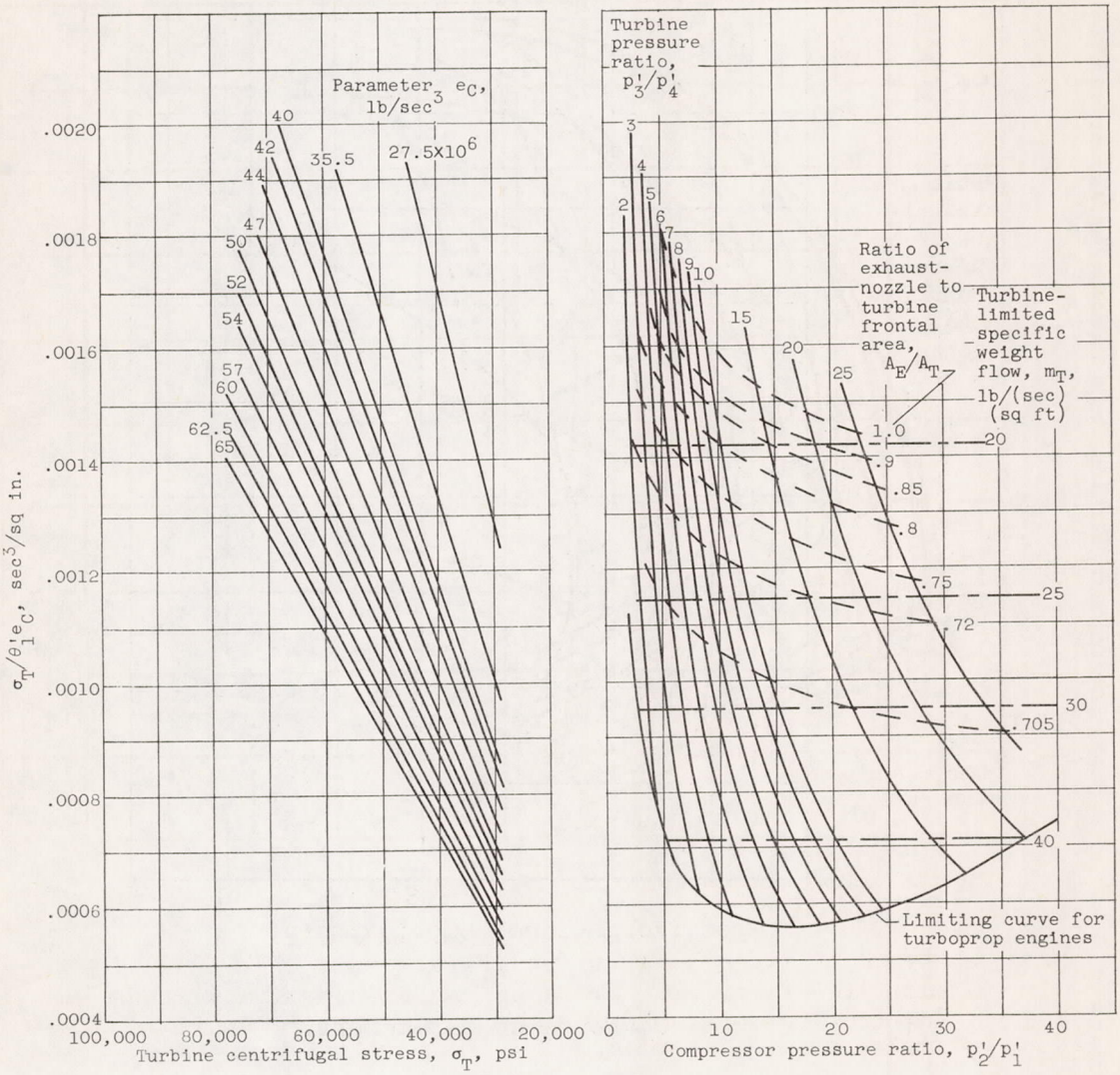

(a) Engine parameters.

Chart VIII. - Turboprop-engine performance. Flight Mach number at tropopause, 0.8; turbine-inlet temperature, 1760° R; engine temperature ratio, 4.

4078

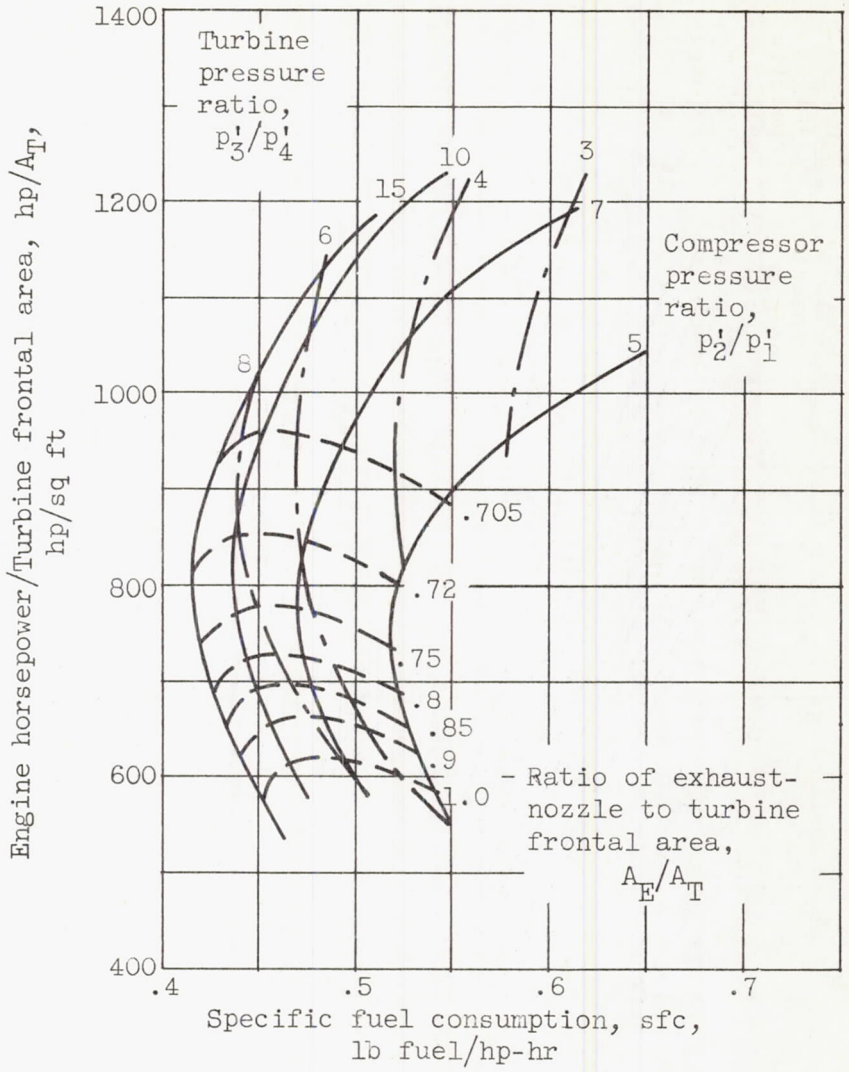

(b) Performance parameters.

Chart VIII. - Concluded. Turboprop-engine performance. Flight Mach number at tropopause, 0.8; turbine-inlet temperature, 1760° R; engine temperature ratio, 4.

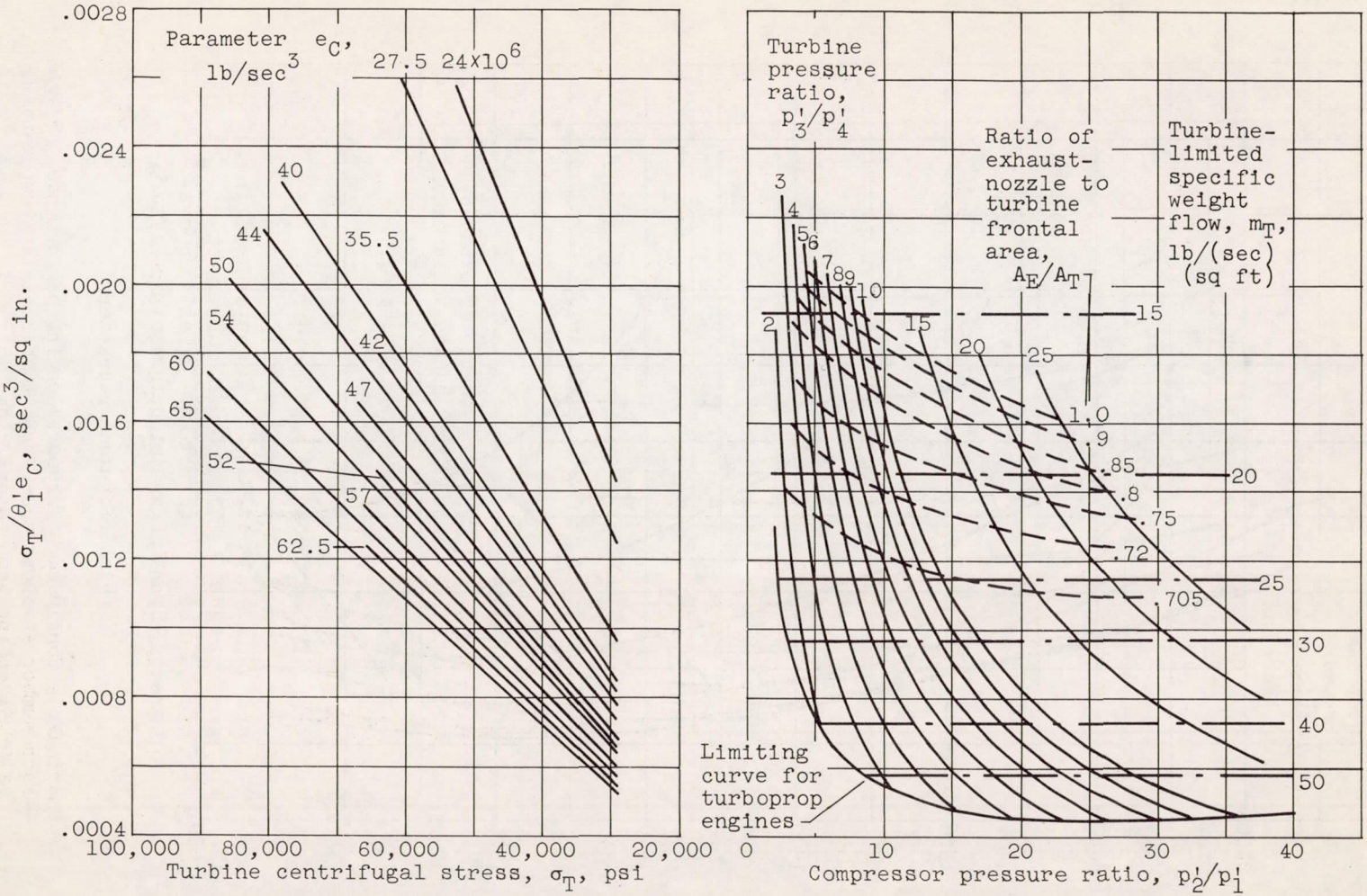

(a) Engine parameters.

Chart IX. - Turboprop-engine performance. Flight Mach number at tropopause, 0.8; turbine-inlet temperature, 2200° R; engine temperature ratio, 5.

4078

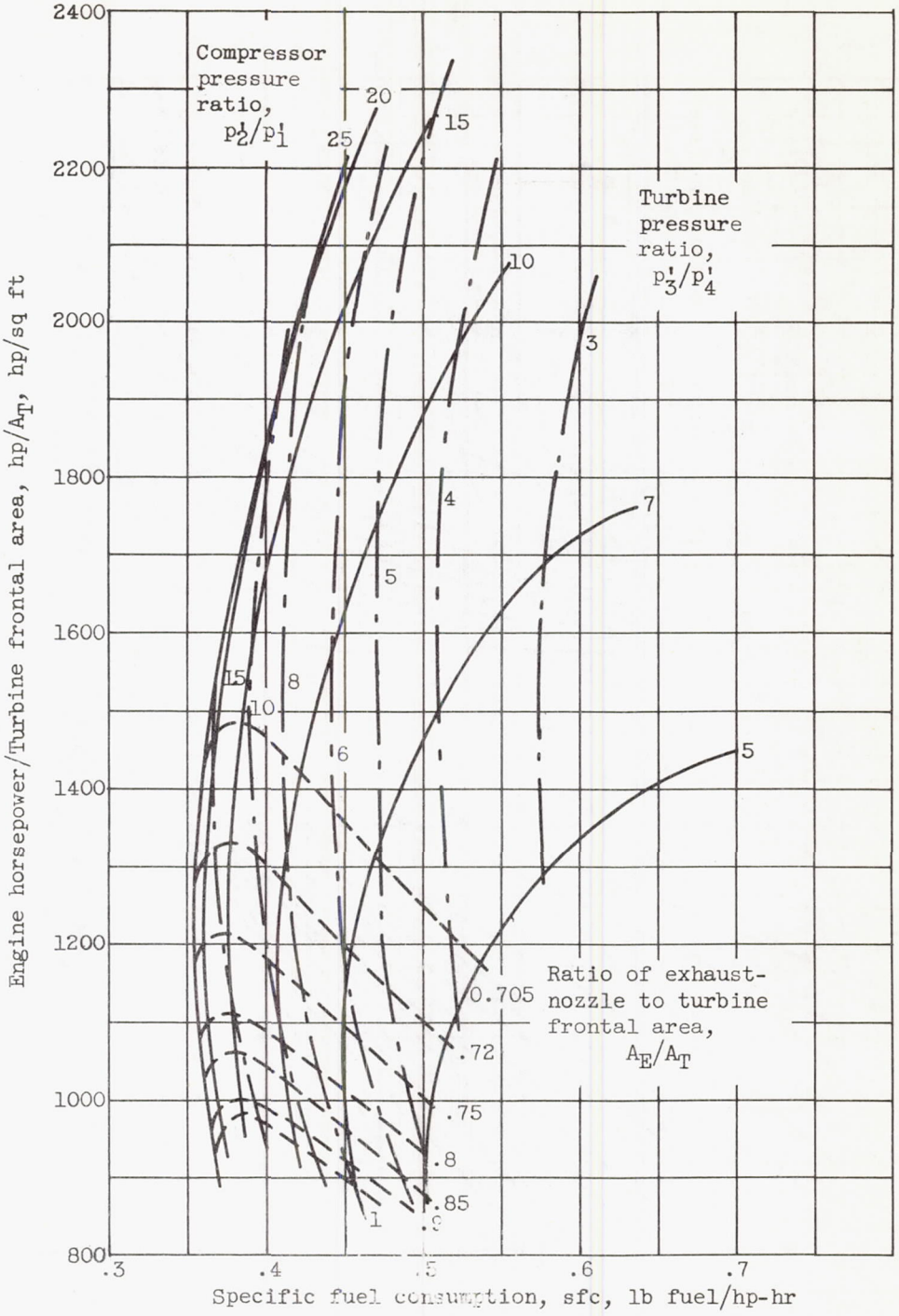

(b) Performance parameters.

Chart IX. - Concluded. Turboprop-engine performance. Flight Mach number at tropopause, 0.8; turbine-inlet temperature, 2200° R; engine temperature ratio, 5.

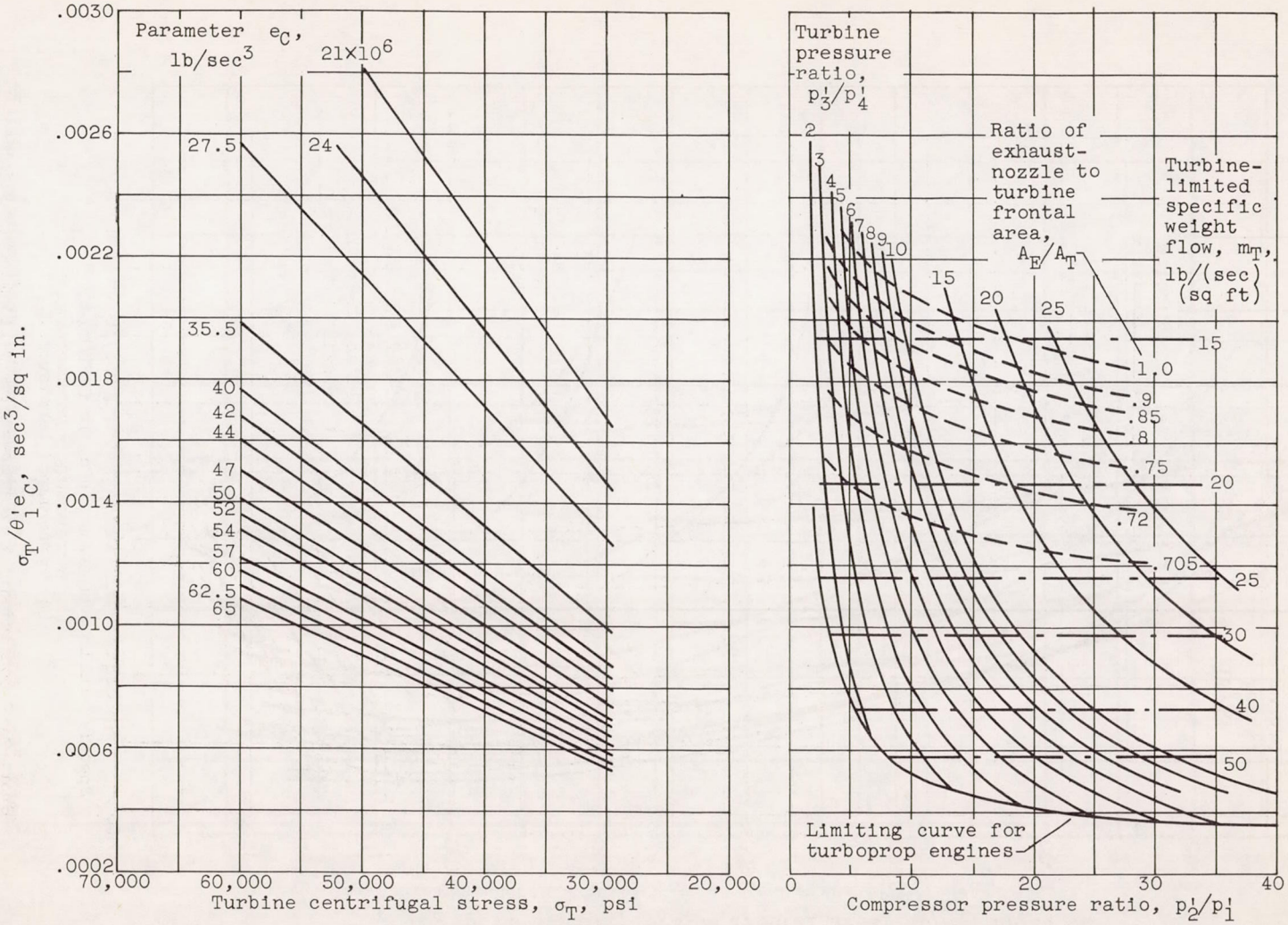

(a) Engine parameters.

Chart X. - Turboprop-engine performance. Flight Mach number at tropopause, 0.8; turbine-inlet temperature, 2641° R; engine temperature ratio, 6.

4078

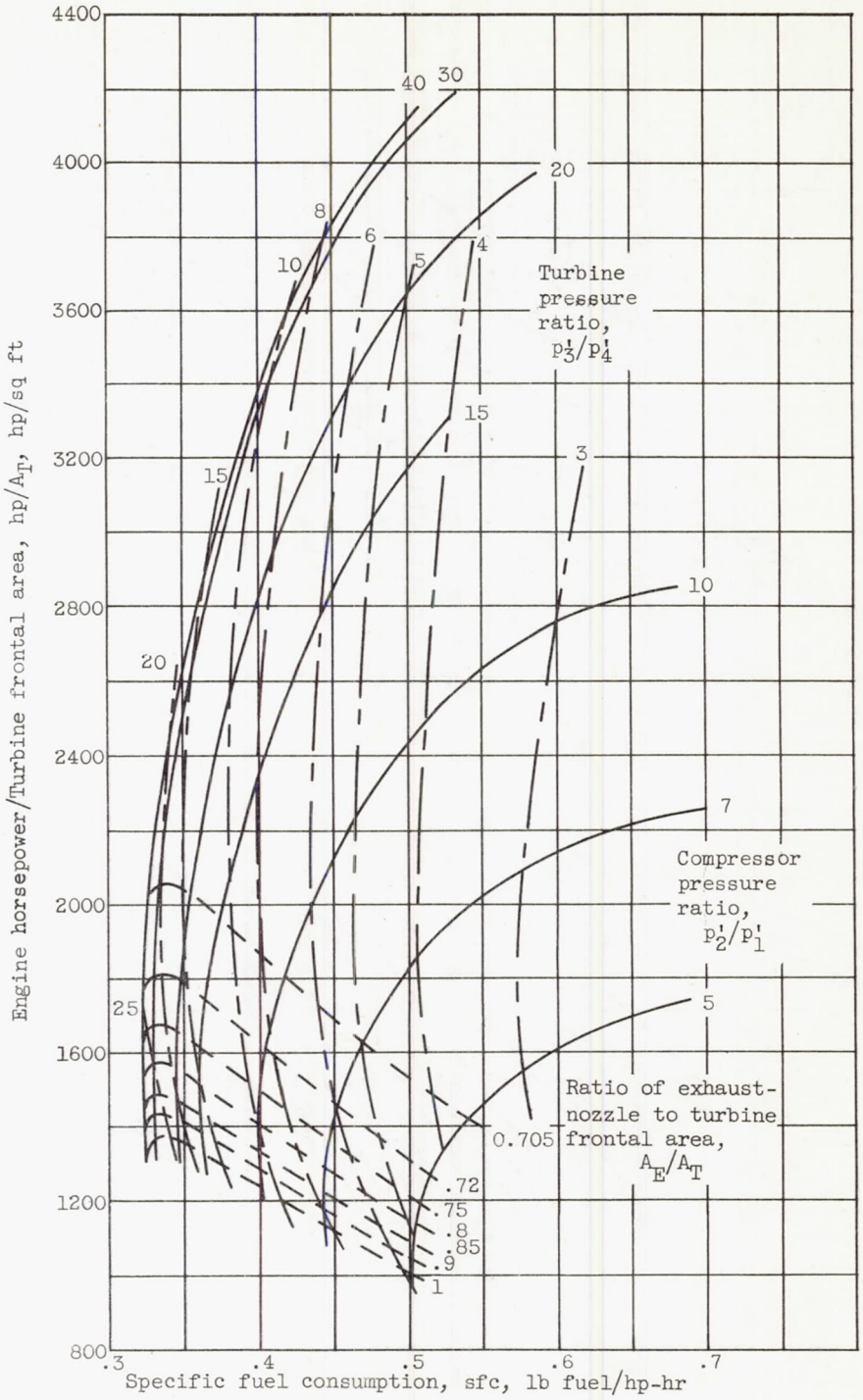

(b) Performance parameters.

Chart X. - Concluded. Turboprop-engine performance. Flight Mach number at tropopause, 0.8; turbine-inlet temperature, 2641° R; engine temperature ratio, 6.

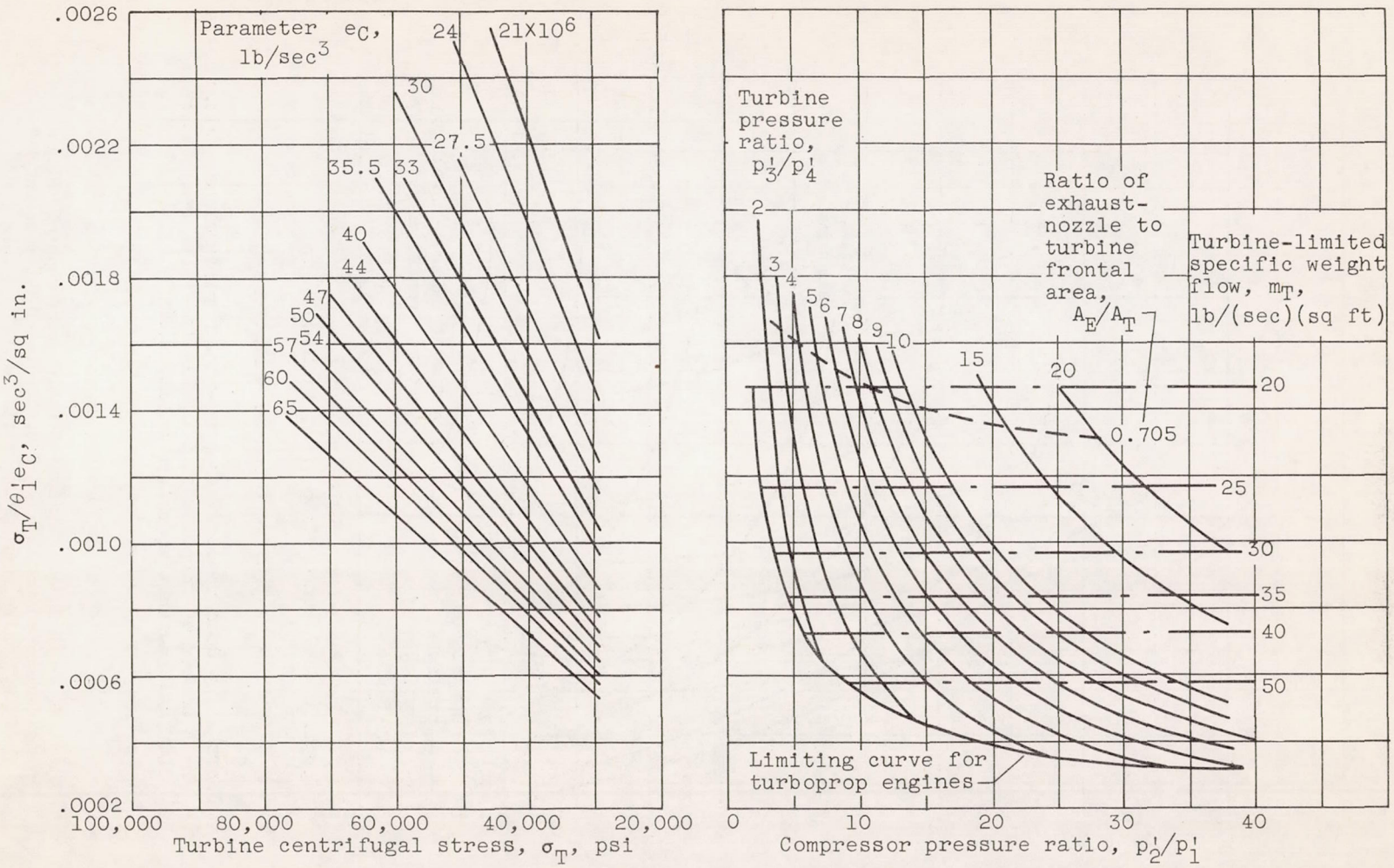

(a) Engine parameters.

Chart XI. - Turboprop-engine performance. Flight Mach number at tropopause, 0.8; turbine-inlet temperature, 3000° R; engine temperature ratio, 6.82.

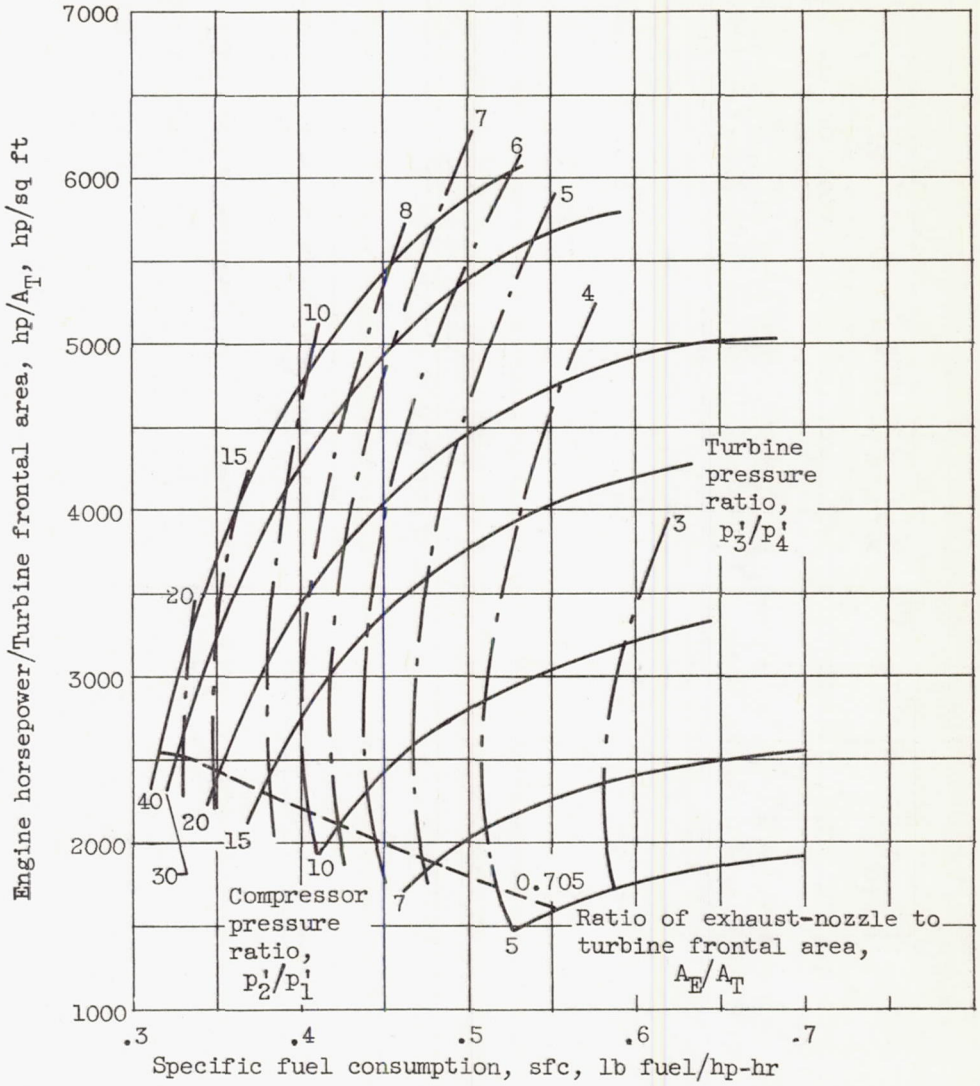

(b) Performance parameters.

Chart X1. - Concluded. Turboprop-engine performance. Flight Mach number at tropopause, 0.8; turbine-inlet temperature, 3000° R; engine temperature ratio, 6.82.